

# Chiral perturbation theory and Bose-Einstein condensation in QCD

Jens O. Andersen,<sup>1,2,\*</sup> Martin Kjøllestad Johnsrud,<sup>1,3,†</sup> Qing Yu,<sup>4,‡</sup> and Hua Zhou<sup>4,§</sup>

<sup>1</sup>*Department of Physics, Faculty of Natural Sciences, NTNU,*

*Norwegian University of Science and Technology, Høgskoleringen 5, N-7491 Trondheim, Norway*

<sup>2</sup>*Niels Bohr International Academy, Blegdamsvej 17, DK-2100 Copenhagen, Denmark*

<sup>3</sup>*Department of Living Matter Physics, Max Planck Institute of Dynamics and Self-Organization, Am Fassberg 17, DE-37077 Göttingen, Germany*

<sup>4</sup>*School of Mathematics and Physics, Southwest University of Science and Technology, Mianyang 621010, China*

(Dated: February 11, 2025)

We present recent results in three-flavor chiral perturbation theory at finite isospin  $\mu_I$  and strangeness  $\mu_S$  chemical potentials at zero temperature. The tree-level spectrum for the mesons and gauge bosons in the pion-condensed phase is derived. The phase diagram to  $\mathcal{O}(p^2)$  in the  $\mu_I$ - $\mu_S$  plane is mapped out with and without electromagnetic effects. The phase diagram consists of a vacuum phase and three Bose-condensed phases with condensates of  $\pi^\pm$ ,  $K^\pm$ , and  $K^0/\bar{K}^0$ , respectively. Including electromagnetic interactions, the charged Bose-condensed phases become Higgs phases via the Higgs mechanism. We calculate the pressure, energy density, isospin density, and speed of sound in the pion-condensed phase to  $\mathcal{O}(p^4)$ . The results are compared with recent lattice simulations and the agreement is very good for isospin chemical potentials up to approximately 180 MeV. Moreover, by integrating out the  $s$ -quark, we show that the thermodynamic quantities can be mapped onto their two-flavor counterparts with renormalized parameters. The breaking of the U(1) symmetry in the Bose-condensed phases gives rise to a Goldstone boson, whose dispersion is linear for small momenta. We use Son's prescription to construct an effective theory for the Goldstone mode in the pion-condensed phase, which is valid for momenta  $p \ll \mu_I$ . It is shown that its damping rate is of order  $p^5$  in the nonrelativistic limit, which is Beliaev's result for a dilute Bose gas. It is also shown that in the nonrelativistic limit the energy density can be matched onto the classic result by Lee, Huang and Yang (LHY) for a dilute Bose, with an  $s$ -wave scattering length that includes radiative corrections.

## I. INTRODUCTION

The phase diagram of quantum chromodynamics (QCD) has received a lot of attention in recent years due to its relevance for the early universe, heavy-ion collisions, and compact stars [1–3]. Conventionally, the phase diagram is shown in the plane of temperature  $T$  and baryon chemical potential  $\mu_B$ , see Fig. 1.

At finite  $\mu_B$ , the sign problem of QCD poses a serious challenge. The fact that the fermion determinant is complex prohibits the use of importance sampling techniques in lattice simulations, which precludes the study of a large part of the phase diagram by this method. However, by expanding the partition function in powers of  $\mu_B/T$  around zero, one can move away from the temperature axis into the  $\mu_B$ - $T$  plane, but obviously not too far. The low- $T$ , high- $\mu_B$  part of the phase diagram has therefore been mapped out by low-energy models that share some of the properties of QCD, for example the Nambu-Jona-Lasinio (NJL), quark-meson (QM) model, and their Polyakov-loop extended counterparts. This is exactly the part that is relevant for compact stars. Some aspects of the phase diagram are indicated in Fig. 1 in the  $\mu_B$ - $T$  plane, for example there may be a quarkyonic phase and

a region where QCD is a color superconductor. This part of the phase diagram is possibly very rich with a number of phases such as the color-flavor locked (CFL) phase, the two-flavor color superconducting (2SC) phase, and Larkin-Ovchinnikov-Fulde-Ferrel (LOFF) phases. Only the existence of the CFL phase, however, is a rigorous result due to asymptotic freedom. For example the existence of the 2SC phase between the CFL phase and normal quark matter depends heavily on model parameters [4–7].

Instead of using a common quark chemical potential  $\mu = \frac{1}{3}\mu_B$  for the different flavors  $f = u, d, s$ , one can introduce an independent chemical potential  $\mu_f$  for each of them. They are expressed in terms of the baryon, isospin, and strangeness chemical potentials as  $\mu_B = \frac{3}{2}(\mu_u + \mu_d)$ ,  $\mu_I = (\mu_u - \mu_d)$ , and  $\mu_S = \frac{1}{2}(\mu_u + \mu_d - 2\mu_s)$ .<sup>1</sup> In the special case  $\mu_u = -\mu_d \neq 0$  and  $\mu_s = 0$ , only the isospin chemical potential  $\mu_I$  is nonzero. From a theoretical point of view, QCD at zero baryon and strangeness chemical potentials, but nonzero isospin chemical potential has the advantage that there is no sign problem: the fermion determinant is (manifestly) real and one can use standard importance sampling techniques to perform lattice simulations of the system. This opens up the possibil-

\* jens.andersen@ntnu.no

† martin.johnsrud@ds.mpg.de

‡ yuq@swust.edu.cn

§ zhouhua@swust.edu.cn

<sup>1</sup> This gives rise to a complicated three-dimensional phase diagram. In recent years, yet another aspect of the QCD phase diagram has been studied in detail, namely the effects of a strong magnetic background  $B$ .

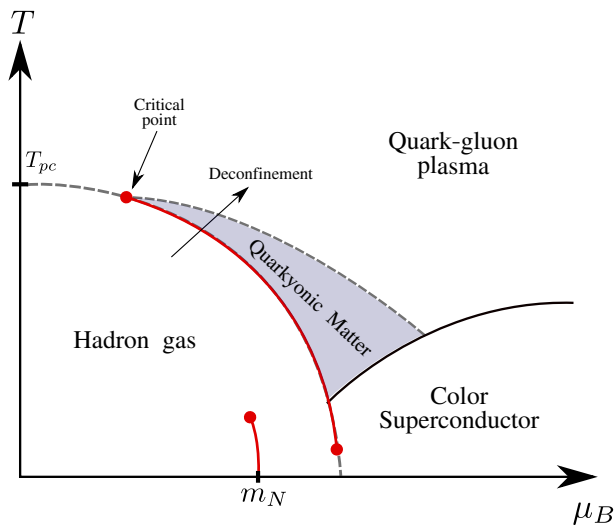


FIG. 1. Schematic phase diagram of QCD in the  $\mu_B$ - $T$  plane. See main text for details.

ity to compare lattice with low-energy effective theories such as chiral perturbation theory and models such as the NJL model and the QM model. Chiral perturbation theory [8–10], first considered at finite  $\mu_I$  in Refs. [11–13], is of particular interest since it gives model-independent predictions. Within its domain of validity, a comparison with lattice results can also be considered a check of the latter.

The first simulations of two-flavor QCD at nonzero isospin chemical potential were performed more than twenty years ago using quenched lattice QCD [14], which later was improved by including dynamical fermions [15, 16] on relatively coarse lattices. Later, the simulations were extended to three-flavor QCD in the phase-quenched approximation [17, 18]. In recent years, high-precision lattice simulations have been carried out [19–25] and the phase diagram in the  $\mu_I$ - $T$  plane has been mapped out, see Fig. 2 (see also Ref. [26] for a determination of the equation of state at finite  $\mu_I$ ). The solid black line is the phase boundary between the hadronic phase and the Bose-condensed phase, where the  $U(1)_{I_3}$  symmetry is broken. The grey dashed line is the phase boundary between the confined and the deconfined phases. For large  $T$  and small  $\mu_I$ , this is the usual transition to a quark-gluon plasma.

It has been shown both on the lattice and in  $\chi$ PT that the transition at  $T = 0$  from the vacuum phase to the pion-condensed phase takes place at a critical isospin chemical potential equal to the physical charged pion mass,  $\mu_I^c = m_{\pi^\pm}$  and that the transition is second order. The transition remains second order at finite  $T$  along the solid black line. Moreover, the vacuum phase exhibits the so-called Silver-Blaze property, meaning that the thermodynamic properties at  $T = 0$  are independent of the chemical potential  $\mu_I$  all the way up to the onset of Bose-Einstein condensation [27]. For asymptotically large values of  $\mu_I$ , quarks rather than pions are the rele-

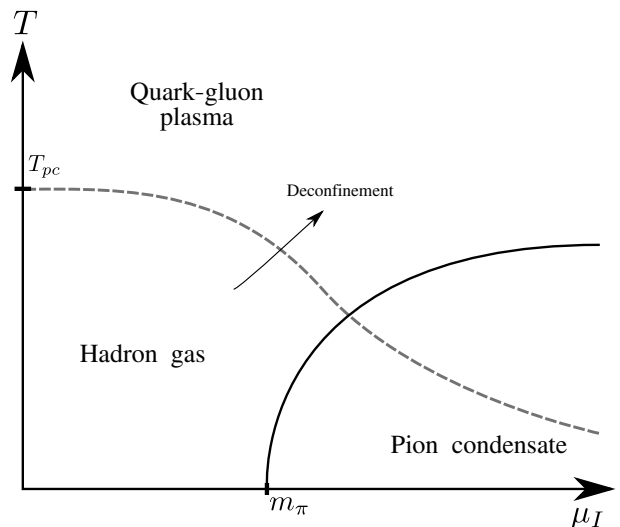


FIG. 2. Schematic phase diagram of QCD in the  $\mu_I$ - $T$  plane. See main text for details.

vant degrees of freedom. Without interactions and at low temperature, the system is described in terms of a Fermi surface. Turning on interactions, the Fermi surface is rendered unstable due to an attractive interaction channel provided by one-gluon exchange. The system then becomes a color superconductor, which is characterized by a BCS gap [11]. At lower densities, the interactions are presumably mediated by instantons. The transition from the BEC phase to the BCS phase is a crossover since the quantum numbers of the condensates are the same. This picture is supported by lattice simulations [23, 24] and the crossover is indicated by the dashed line to the right in Fig. 2. Various aspects of QCD at finite isospin can be found in e.g. Refs. [11–13, 28–33] ( $\chi$ PT), [34–39] (NJL model), and [40–44] (QM model). Ref. [45] provides an application of  $\chi$ PT in an external magnetic field at finite  $\mu_I$ , and a review on meson condensation in QCD can be found in Ref. [46].

Electromagnetic interactions in chiral perturbation theory were first included at the leading-order (LO) by Ecker et al. [47] and at the next-to leading-order (NLO) by Urech [48]. In Ref. [48], the NLO Lagrangian was derived and the leading corrections to the meson masses were computed, i.e. corrections to Dashen’s theorem [49]. Other early applications of  $\chi$ PT to e.g. scattering of pions can be found in Refs. [50–52]. In the context of chiral perturbation theory, electromagnetic effects have not yet been included at finite chemical potentials. Since the spontaneously broken  $U(1)_{I_3}$  symmetry group in the pion-condensed phase implies the breaking of the local gauge symmetry of electromagnetism, the Goldstone boson disappears from the physical spectrum and the photon becomes massive via the Higgs mechanism. The pion-condensed phase is then a superconductor and QCD is in a Higgs phase. The same remark applies to the phase of condensed charged kaons, but not to the phase of con-

densed neutral kaons. In this case, the phase is a superfluid.

The paper is organized as follows. In Sec. II, we discuss chiral perturbation theory including chemical potentials as well as electromagnetic interactions. In Sec. III, the relations between the thermodynamic potential and various thermodynamic quantities are briefly reviewed. In Sec. IV, we discuss the form of the QCD ground state as a function of the chemical potentials and how to parametrize the fluctuations around it. The leading-order results for the quasi-particle masses, thermodynamic quantities, and the phase diagram are presented in Sec. V. In Sec. VI, we calculate the pressure, isospin density, energy density, and the speed of sound to the next-to leading order without electromagnetic interactions. The results are compared with recent lattice simulations. We also show how the three-flavor result for the pressure reduces to the two-flavor result with renormalized couplings. In Sec. VII, the pressure is calculated to the next-to-next-to leading order (NNLO) in the chiral limit. The low-energy effective theory for the Goldstone bosons is discussed in Sec. VIII, where we calculate their damping rate in the nonrelativistic limit. In Sec. IX, the dilute Bose gas is reviewed. We show that the nonrelativistic limit of  $\chi$ PT reproduces the results for the dilute Bose gas with a renormalized  $s$ -wave scattering length. Finally, we summarize in Sec. X.

## II. CHIRAL PERTURBATION THEORY

In this section, we briefly discuss the construction of the low-energy chiral Lagrangian using the coset construction. This has been done in detail many times in the literature. Some of the original references are [53, 54], while more recent introductions to effective field theory can be found in Refs. [55–57]. The QCD Lagrangian with  $N_f$  massless quarks has an  $SU(N_f)_L \times SU(N_f)_R$  global symmetry which in the vacuum is broken down to  $SU(N_f)_V$  by the quark condensate. The vacuum manifold or the coset is then  $SU(N_f)_L \times SU(N_f)_R / SU(N_f)_V$ . The vacuum manifold of the effective low-energy theory can be parametrized as

$$\Sigma = \Sigma_0 e^{i\phi_a X_a / f}, \quad (1)$$

where  $\Sigma_0$  is the vacuum state,  $X_a$  are the broken symmetry generators,  $\phi_a$  are the Goldstone fields, and  $f$  is the bare pion decay constant. For two flavors, the broken generators are the Pauli matrices  $\tau_a$  and in the three-flavor case, the broken generators are the Gell-Mann matrices  $\lambda_a$ . They are normalized as  $\langle \tau_a \tau_b \rangle = \langle \lambda_a \lambda_b \rangle = 2\delta_{ab}$ , where  $\langle A \rangle$  denotes the trace of the matrix  $A$ . Under  $SU(N_f)_L \times SU(N_f)_R$  transformations  $L$  and  $R$ ,  $\Sigma$  transforms as

$$\Sigma \rightarrow \Sigma' = L \Sigma R^\dagger. \quad (2)$$

The fundamental object or building block in the coset construction is the so-called Maurer-Cartan form

$$d_\mu = i\Sigma^\dagger \partial_\mu \Sigma, \quad (3)$$

which is an element of the  $\mathfrak{su}(N_f)$  algebra. One constructs the invariant terms in the Lagrangian by taking traces of products of Eq. (3). Each factor of  $d_\mu$  counts as one power of momentum via the derivative of  $\Sigma$ . The leading term  $\langle d_\mu \rangle$  clearly vanishes since the generators of  $SU(N_f)$  are traceless. The next term is the trace of a product of two  $d_\mu$ 's with indices contracted so it is Lorentz invariant. At leading order in the low-energy expansion, the Lagrangian is therefore

$$\mathcal{L}_2 = \frac{1}{4} f^2 \langle \partial_\mu \Sigma^\dagger \partial^\mu \Sigma \rangle. \quad (4)$$

In real-world QCD, the current quark masses  $m_f$  are nonzero. This explicit symmetry breaking in the QCD Lagrangian gives rise to the symmetry-breaking terms in the chiral Lagrangian. Similarly, electroweak interactions also break chiral symmetry. For example, we cannot rotate a  $u$  quark into a  $d$  quark since they have different electric charges. Finally, for each intact global symmetry, we may introduce an independent chemical potential  $\mu_i$  in the QCD Lagrangian. However, this can be done simultaneously for  $\mu_i$  and  $\mu_j$  only if the corresponding charges commute. In QCD, we can introduce an independent chemical potential  $\mu_f$  for each quark flavor  $f$  ( $f = u, d, s$ ). In order to incorporate these effects in the chiral Lagrangian, it is convenient to couple the QCD Lagrangian to external fields  $v_\mu$ ,  $a_\mu$ ,  $s$ , and  $p$  as [9, 48]

$$\begin{aligned} \mathcal{L}_{\text{QCD}} = & -\frac{1}{4} G_{\mu\nu}^a G_a^{\mu\nu} + i\bar{q}\gamma^\mu D_\mu q + \bar{q}\gamma^\mu (v_\mu + \gamma^5 a_\mu) q \\ & -\bar{q}(s - i\gamma^5 p)q. \end{aligned} \quad (5)$$

Here,  $G_{\mu\nu}^a$  is the nonabelian field-strength tensor and  $D_\mu = \partial_\mu - igT_a \mathcal{A}_\mu^a$  is the corresponding covariant derivative where  $g$  is the QCD strong coupling constant,  $T_a$  are the  $SU(3)_c$  generators and  $\mathcal{A}_\mu^a$  are the gluon fields. The external fields are then evaluated at nonvanishing values corresponding to the symmetry-breaking terms. These are

$$s = M = \text{diag}(m_u, m_d, m_s), \quad (6)$$

$$p = -\lambda_a j, \quad (7)$$

$$l_\mu = v_\mu - a_\mu = \delta_{0\mu} \text{diag}(\mu_u, \mu_d, \mu_s) + Q_L A_\mu, \quad (8)$$

$$r_\mu = v_\mu + a_\mu = \delta_{0\mu} \text{diag}(\mu_u, \mu_d, \mu_s) + Q_R A_\mu, \quad (9)$$

The source  $s$  accounts for the quark masses, while  $A_\mu$  is the electromagnetic field, and  $\mu_f$  accounts for finite density. The pseudoscalar source  $p$  is needed if we want to calculate a Bose condensate. We choose  $a = 2, 5$ , or  $7$  depending on the condensate of interest,  $\pi^\pm$ ,  $K^\pm$  or  $K^0/\bar{K}^0$ , see Subsec. IV A. Instead of the quark chemical potentials  $\mu_f$ , we can introduce the baryon, isospin, and

strangeness chemical potentials  $\mu_B$ ,  $\mu_I$ , and  $\mu_S$  using

$$\text{diag}(\mu_u, \mu_d, \mu_s) = \frac{1}{3}(\mu_B - \mu_S)\mathbb{1} + \frac{1}{2}\mu_I\lambda_3 + \frac{1}{\sqrt{3}}\mu_S\lambda_8, \quad (10)$$

with

$$\mu_B = \frac{3}{2}(\mu_u + \mu_d), \quad (11)$$

$$\mu_I = \mu_u - \mu_d, \quad (12)$$

$$\mu_S = \frac{1}{2}(\mu_u + \mu_d - 2\mu_s). \quad (13)$$

The  $SU(3)_L \times SU(3)_R$  invariance in QCD can be made local provided the left-handed and right-handed fields  $q_L$  and  $q_R$ , the external fields transform, and the charge matrices as

$$q_L \rightarrow Lq_L, \quad (14)$$

$$q_R \rightarrow Rq_R, \quad (15)$$

$$(s + ip) \rightarrow R(s + ip)L^\dagger, \quad (16)$$

$$l_\mu \rightarrow Ll_\mu L^\dagger + iL\partial_\mu L^\dagger, \quad (17)$$

$$r_\mu \rightarrow Rr_\mu R^\dagger + iR\partial_\mu R^\dagger, \quad (18)$$

$$Q_L \rightarrow LQ_L L^\dagger, \quad (19)$$

$$Q_R \rightarrow RQ_R R^\dagger. \quad (20)$$

In the effective theory, the local invariance is implemented by replacing a partial derivative by a covariant derivative as

$$\partial_\mu \Sigma \rightarrow \nabla_\mu \Sigma = \partial_\mu \Sigma - ir_\mu \Sigma + i\Sigma l_\mu, \quad (21)$$

$$\partial_\mu \Sigma^\dagger \rightarrow \nabla_\mu \Sigma^\dagger = \partial_\mu \Sigma^\dagger + i\Sigma^\dagger r_\mu - i\Sigma^\dagger l_\mu. \quad (22)$$

One can now use the building blocks  $\Sigma$ ,  $\Sigma^\dagger$ ,  $\nabla_\mu \Sigma$ ,  $\nabla_\mu \Sigma^\dagger$ , and  $s \pm ip$  to construct invariant terms. Of course, the external fields do not transform according to Eqs. (14)–(20), once they take the constant values, the symmetries are explicitly broken. However, by construction, the symmetries in the effective theory are broken in the same way as in QCD. For example, setting  $Q_R = Q_L = Q = e \text{diag}(\frac{2}{3}, -\frac{1}{3}, -\frac{1}{3})$  being the quark charge matrix, ensures that electromagnetic interactions break the flavor symmetry in the correct way. As mentioned above, one can introduce as many independent chemical potentials as there are commuting charges [58, 59], which in  $\chi$ PT is the dimension of the Cartan subalgebra. For  $SU(3)$ , the subalgebra consists of  $\lambda_3$  and  $\lambda_8$  and we can introduce  $\mu_I$  and  $\mu_S$ . The introduction of the chemical potentials via Eq. (10) breaks  $SU(3)_V$  down to  $U(1)_{I_3} \times U(1)_S$ . The baryon chemical potential is redundant in  $\chi$ PT since the mesons have zero baryon charge,  $\Sigma$  transforms trivially under  $U(1)_B$ , and the thermodynamic potential is independent of  $\mu_B$ .

There are other choices that may be convenient when discussing kaon condensation in QCD. Eq. (10) can be

written as

$$\text{diag}(\mu_u, \mu_d, \mu_s) = \frac{1}{3}(\mu_B - \mu_S)\mathbb{1} + \frac{1}{2}\mu_{K^\pm}\lambda_Q + \frac{1}{2}\mu_{K^0}\lambda_K, \quad (23)$$

where  $\lambda_Q = \lambda_3 + \frac{1}{\sqrt{3}}\lambda_8$  and  $\lambda_K = -\lambda_3 + \frac{1}{\sqrt{3}}\lambda_8$  and the corresponding chemical potentials are  $\mu_{K^\pm} = \frac{1}{2}\mu_I + \mu_S$  and  $\mu_{K^0} = -\frac{1}{2}\mu_I + \mu_S$ , respectively. These are the combinations of  $\mu_I$  and  $\mu_S$  that correspond to the quark content of the charged and neutral kaons. When the absolute value of  $\mu_{K^\pm}$  or  $\mu_{K^0}$  exceeds the corresponding kaon mass, the kaon forms a Bose condensate.

The organization of the effective Lagrangian in a systematic low-energy expansion requires a consistent power-counting scheme. The original scheme of Gasser and Leutwyler [9, 10], which does not include electromagnetic interactions, is such that a covariant derivative counts as  $\mathcal{O}(p)$ . The leading derivative term is already given in Eq. (4), but there is another term of order  $p^2$ , proportional to  $\langle \Sigma^\dagger \chi + \chi^\dagger \Sigma \rangle$ , where  $\chi = 2B_0(s + ip)$  and  $B_0$  is a constant related to the quark condensate. The leading-order Lagrangian is then

$$\mathcal{L}_2 = \frac{1}{4}f^2 \langle \nabla_\mu \Sigma^\dagger \nabla^\mu \Sigma \rangle + \frac{1}{4}f^2 \langle \Sigma^\dagger \chi + \chi^\dagger \Sigma \rangle. \quad (24)$$

If we include electromagnetic terms, we need additional counting rules, which were provided by Urech [48]. Since the covariant derivative is of order  $p$ , the term  $QA_\mu$  is also of order  $p$ . The charge  $e$  and the field  $A_\mu$  are assigned to be of order  $p$  and order one, respectively. This rule does not alter the standard chiral counting. In addition to including  $A_\mu$  in the covariant derivative above, there is a new invariant term of the form  $\langle Q_L \Sigma Q_R \Sigma^\dagger \rangle^2$  such that the leading-order Lagrangian is

$$\mathcal{L}_2 = -\frac{1}{4}F_{\mu\nu}F^{\mu\nu} + \frac{1}{4}f^2 \langle \nabla_\mu \Sigma^\dagger \nabla^\mu \Sigma \rangle + \frac{1}{4}f^2 \langle \Sigma^\dagger \chi + \chi^\dagger \Sigma \rangle + C \langle Q \Sigma Q \Sigma^\dagger \rangle + \mathcal{L}_{\text{gf}} + \mathcal{L}_{\text{ghost}} - eA_\mu J_{\text{back}}^\mu, \quad (25)$$

where the first term is the kinetic term for the photons,  $C$  is a coupling constant and the gauge-fixing Lagrangian in general  $R_\xi$  gauge is

$$\mathcal{L}_{\text{gf}} = -\frac{1}{2\xi}(\partial_\mu A^\mu + \xi e f \sin \alpha \phi_1)^2, \quad (26)$$

where  $\xi$  is the gauge parameter. Denoting the ghost field by  $c$ , the ghost Lagrangian is

$$\mathcal{L}_{\text{ghost}} = \partial_\mu \bar{c} \partial^\mu c - \xi e^2 f^2 \sin^2 \alpha \bar{c} c + \xi e^2 f \sin \alpha \phi_1 \bar{c} c \quad (27)$$

Finally, the last term is the coupling of the gauge field to background charges and currents  $J_{\text{back}}^\mu$ . This term is

<sup>2</sup> This term breaks the flavor symmetries once we set  $Q_L = Q_R = Q$ , as explained below Eq. (22).

necessary to ensure overall electric neutrality [58]. We will not need it in the remainder of the paper.

At next-to-leading order, there are many more terms in the chiral Lagrangian. For general  $SU(N)$ , there are 13 independent terms in addition to contact terms (contact terms are terms that depend only on the external fields). For two flavors, there are 10 terms and an additional 14 terms if we include electromagnetism [9, 50, 51]. For three flavors the number of operators are 12 and 17, respectively [10, 48]. The reduction in the number of terms for  $N_f = 2$  and  $N_f = 3$  is due to the fact that not all terms in the  $SU(N_f)$  case are linearly independent. Not all of the terms in the  $N_f = 2$  and  $N_f = 3$  case are relevant to the present work. Ignoring electromagnetic effects, the operators we need in the three-flavor case are

$$\begin{aligned} \mathcal{L}_4 = & L_1 \langle \nabla_\mu \Sigma^\dagger \nabla^\mu \Sigma \rangle^2 + L_2 \langle \nabla_\mu \Sigma^\dagger \nabla_\nu \Sigma \rangle \langle \nabla^\mu \Sigma^\dagger \nabla^\nu \Sigma \rangle \\ & + L_3 \langle \nabla_\mu \Sigma^\dagger \nabla^\mu \Sigma \nabla_\nu \Sigma^\dagger \nabla^\nu \Sigma \rangle \\ & + L_4 \langle \nabla_\mu \Sigma^\dagger \nabla^\mu \Sigma \rangle \langle \chi^\dagger \Sigma + \chi \Sigma^\dagger \rangle \\ & + L_5 \langle \nabla_\mu \Sigma^\dagger \nabla^\mu \Sigma \rangle \langle \chi^\dagger \Sigma + \chi \Sigma^\dagger \rangle^2 \\ & + L_6 \langle \chi^\dagger \Sigma + \chi \Sigma^\dagger \rangle^2 + L_7 \langle \chi \Sigma - \chi \Sigma^\dagger \rangle^2 \\ & + L_8 \langle \chi^\dagger \Sigma \chi^\dagger \Sigma + \chi \Sigma^\dagger \chi \Sigma^\dagger \rangle + H_2 \langle \chi \chi^\dagger \rangle. \end{aligned} \quad (28)$$

The parameters  $L_1$ – $L_8$  are low-energy constants, while the parameter  $H_2$  is referred to as a high-energy constant. The relations between the bare and renormalized parameters are

$$L_i = L_i^r - \frac{\Gamma_i (\delta \Lambda)^{-2\epsilon}}{2(4\pi)^2} \frac{1}{\epsilon}, \quad (29)$$

$$H_i = H_i^r - \frac{\Delta_i (\delta \Lambda)^{-2\epsilon}}{2(4\pi)^2} \frac{1}{\epsilon}, \quad (30)$$

where  $\Lambda$  is the renormalization scale and  $\delta$  is a constant.  $\delta = 1$  corresponds to minimal subtraction, while  $\log \delta = -\frac{1}{2}(\log 4\pi - \gamma_E + 1)$  corresponds to the modified minimal subtraction scheme [60]. The constants  $\Gamma_i$  and  $\Delta_i$  assume the following values [10]

$$\Gamma_1 = \frac{3}{32}, \quad \Gamma_2 = \frac{3}{16}, \quad \Gamma_3 = 0, \quad (31)$$

$$\Gamma_4 = \frac{1}{8}, \quad \Gamma_5 = \frac{3}{8}, \quad \Gamma_6 = \frac{11}{144}, \quad (32)$$

$$\Gamma_7 = 0, \quad \Gamma_8 = \frac{5}{48}, \quad \Delta_2 = \frac{5}{24}. \quad (33)$$

The renormalized couplings  $L_i^r$  and  $H_i^r$  are scale-dependent and run to ensure the scale independence of observables in  $\chi$ PT. Since the bare couplings are independent of  $\Lambda$ , differentiation of Eqs. (29)–(30) with respect to the scale yields the renormalization group equations

$$\Lambda \frac{dL_i^r}{d\Lambda} = -\frac{\Gamma_i (\delta \Lambda)^{-2\epsilon}}{(4\pi)^2}, \quad \Lambda \frac{dH_i^r}{d\Lambda} = -\frac{\Delta_i (\delta \Lambda)^{-2\epsilon}}{(4\pi)^2}. \quad (34)$$

We note that  $\Gamma_3 = \Gamma_7 = 0$ , which implies that  $L_3^r$  and  $L_7^r$  do not run, we therefore write  $L_3 = L_3^r$  and  $L_7 = L_7^r$ .

The solutions to the renormalization group equations are

$$L_i^r(\Lambda) = L_i^r(\Lambda_0) + \frac{\Gamma_i}{2(4\pi)^2} \frac{1}{\epsilon} [(\delta \Lambda)^{-2\epsilon} - (\delta \Lambda_0)^{-2\epsilon}] \quad (35)$$

$$H_i^r(\Lambda) = H_i^r(\Lambda_0) + \frac{\Delta_i}{2(4\pi)^2} \frac{1}{\epsilon} [(\delta \Lambda)^{-2\epsilon} - (\delta \Lambda_0)^{-2\epsilon}] \quad (36)$$

where  $\Lambda_0$  is a reference scale. In the limit  $\epsilon \rightarrow 0$ , the solutions reduce to

$$L_i^r(\Lambda) = L_i^r(\Lambda_0) - \frac{\Gamma_i}{2(4\pi)^2} \log \frac{\Lambda^2}{\Lambda_0^2}, \quad (37)$$

$$H_i^r(\Lambda) = H_i^r(\Lambda_0) - \frac{\Delta_i}{2(4\pi)^2} \log \frac{\Lambda^2}{\Lambda_0^2}. \quad (38)$$

In the two-flavor case, the relevant terms in NLO Lagrangian are <sup>3</sup>

$$\begin{aligned} \mathcal{L}_4 = & \frac{1}{4} l_1 \langle \nabla_\mu \Sigma^\dagger \nabla^\mu \Sigma \rangle^2 + \frac{1}{4} l_2 \langle \nabla_\mu \Sigma^\dagger \nabla_\nu \Sigma \rangle \langle \nabla^\mu \Sigma^\dagger \nabla^\nu \Sigma \rangle \\ & + \frac{1}{16} (l_3 + l_4) \langle \chi^\dagger \Sigma + \Sigma^\dagger \chi \rangle^2 \\ & + \frac{1}{8} l_4 \langle \nabla_\mu \Sigma^\dagger \nabla^\mu \Sigma \rangle \langle \chi^\dagger \Sigma + \Sigma^\dagger \chi \rangle \\ & - \frac{1}{16} l_7 \langle \chi^\dagger \Sigma - \Sigma^\dagger \chi \rangle^2 + \frac{1}{2} h_1 \langle \chi^\dagger \chi \rangle, \end{aligned} \quad (39)$$

where  $l_1$ – $l_4$ ,  $l_7$ , and  $h_1$  are bare coupling constants.<sup>4</sup> The relations between the bare couplings and their renormalized counterparts are

$$l_i = l_i^r - \frac{\gamma_i (\delta \Lambda)^{-2\epsilon}}{2(4\pi)^2} \frac{1}{\epsilon}, \quad (40)$$

$$h_i = h_i^r - \frac{\delta_i \Lambda^{-2\epsilon}}{2(4\pi)^2} \frac{1}{\epsilon}, \quad (41)$$

where  $\gamma_i$  and  $\delta_i$  are pure numbers

$$\gamma_1 = \frac{1}{3}, \quad \gamma_2 = \frac{2}{3}, \quad \gamma_3 = -\frac{1}{2}, \quad (42)$$

$$\gamma_4 = 2, \quad \gamma_7 = 0, \quad \delta_1 = 0. \quad (43)$$

The parameters satisfy renormalization group equations similar to Eq. (34) with solutions that specify their running. For  $\epsilon = 0$ , the solution is

$$l_i^r(\Lambda) = \frac{\gamma_i}{2(4\pi)^2} \left[ \bar{l}_i + \log \frac{m_{\pi,0}^2}{\Lambda^2} \right], \quad (44)$$

where  $\bar{l}_i$  are constants. Up to a prefactor these constants equal  $\bar{l}_i^r(\Lambda)$  evaluated at the scale of the (bare) pion mass.

<sup>3</sup> The expression in [9] is written using  $O(4)$  vector notation, instead of the more common  $SU(2)_L \times SU(2)_R$  matrix notation employed in this text. This leads to some additional numerical factors. The conversion is explained in Appendix D of [61].

<sup>4</sup>  $h_1$  in this text corresponds to  $h_1 - l_4$  in [9] due to rewriting of terms [62].

In the two-flavor case, we will be computing the NNLO pressure in the chiral limit in section VII. In this limit,  $m_{\pi,0} \rightarrow 0$ , so in this case we will use the running coupling  $l_i^r(\Lambda)$  instead.

At  $\mathcal{O}(p^6)$ , the Lagrangian contains a larger number of terms, 57 for SU(2) and 94 for SU(3) [60, 63]. Most of them vanish in the chiral limit and for two flavors, the set of operators reduces to

$$\begin{aligned} \mathcal{L}_6 = & C_{24} \langle (\nabla_\mu \Sigma^\dagger \nabla^\mu \Sigma)^3 \rangle \\ & + C_{25} \langle \nabla_\rho \Sigma^\dagger \nabla^\rho \Sigma \nabla_\mu \Sigma^\dagger \nabla_\nu \Sigma \nabla^\mu \Sigma^\dagger \nabla^\nu \Sigma \rangle \\ & + C_{26} \langle \nabla_\mu \Sigma^\dagger \nabla_\nu \Sigma \nabla_\rho \Sigma^\dagger \nabla^\mu \Sigma \nabla^\nu \Sigma^\dagger \nabla^\rho \Sigma \rangle, \end{aligned} \quad (45)$$

where  $C_{24}$ – $C_{26}$  are bare couplings. The relation between the bare couplings  $C_i$  and renormalized couplings  $C_i^r$  is

$$\begin{aligned} C_i = & \frac{C_i^r(\delta\Lambda)^{-4\epsilon}}{f^2} - \frac{\gamma_i^{(2)}(\delta\Lambda)^{-4\epsilon}}{4(4\pi)^4 f^2} \frac{1}{\epsilon^2} \\ & + \frac{(\gamma_i^{(1)} + \gamma_i^{(L)})(\delta\Lambda)^{-4\epsilon}}{2(4\pi)^2 f^2} \frac{1}{\epsilon}, \end{aligned} \quad (46)$$

where  $\gamma_i^{(1)}$  and  $\gamma_i^{(2)}$  are pure numbers. Moreover

$$\gamma_i^{(L)} = \sum_j \gamma_{ij}^{(L)}(\delta\Lambda)^{2\epsilon} l_j^r, \quad (47)$$

where  $\gamma_{ij}^{(L)}$  are also pure numbers. For  $\epsilon = 0$ , the renormalization group equations for the running couplings  $C_i^r(\Lambda)$  read [60]

$$\Lambda \frac{dC_i^r}{d\Lambda} = \frac{1}{(4\pi)^2} \left[ 2\gamma_i^{(1)} + \gamma_i^{(L)} \right]. \quad (48)$$

In section VII, we need the combination  $\mathcal{C} = C_{24} + C_{25} + C_{26}$ , cf. Eq. (45). The relevant coefficients are [60, 63]

$$\gamma_{24}^{(1)} = -\frac{1}{(4\pi)^2} \frac{9}{32}, \quad \gamma_{25}^{(1)} = -\frac{1}{(4\pi)^2} \frac{67}{432}, \quad (49)$$

$$\gamma_{26}^{(1)} = \frac{1}{(4\pi)^2} \frac{449}{864}, \quad \gamma_{24}^{(2)} = -\frac{137}{72}, \quad (50)$$

$$\gamma_{25}^{(2)} = \frac{5}{36}, \quad \gamma_{26}^{(2)} = \frac{55}{72}, \quad (51)$$

$$\gamma_{24}^{(L)} = \left[ -2l_1^r - \frac{16}{3}l_2^r - \frac{5}{4}l_6^r \right], \quad (52)$$

$$\gamma_{25}^{(L)} = \left[ 2l_1^r - \frac{1}{3}l_2^r + \frac{1}{2}l_6^r \right], \quad (53)$$

$$\gamma_{26}^{(L)} = \left[ \frac{8}{3}l_2^r + \frac{3}{4}l_6^r \right]. \quad (54)$$

The renormalized coupling  $\mathcal{C}^r = C_{24}^r + C_{25}^r + C_{26}^r$  satisfies the renormalization group equation

$$\Lambda \frac{d\mathcal{C}^r}{d\Lambda} = \frac{1}{6(4\pi)^4} - \frac{3l_2^r}{(4\pi)^2}. \quad (55)$$

The solution to this equation is

$$\begin{aligned} \mathcal{C}^r(\Lambda) = & \mathcal{C}^r(\Lambda_0) - \frac{3}{2(4\pi)^2} \log \frac{\Lambda^2}{m_{\pi,0}^2} \\ & \times \left[ l_2^r(\Lambda) + \frac{1}{6(4\pi)^2} \left( \log \frac{\Lambda^2}{m_{\pi,0}^2} - \frac{1}{3} \right) \right]. \end{aligned} \quad (56)$$

In the calculation of the thermodynamic quantities in  $\chi$ PT, we encounter a number of one and two-loop integrals. Some of these integrals are ultraviolet divergent and we use dimensional regularization to regulate them. We introduce the following notation for the integrals in Euclidean space

$$\int_P = \int_{-\infty}^{\infty} \frac{dp_0}{2\pi} \int_p, \quad (57)$$

where

$$\int_p = \Lambda^{2\epsilon} \int \frac{d^d p}{(2\pi)^d}, \quad (58)$$

with  $P = (p_0, \mathbf{p})$ ,  $p = |\mathbf{p}|$  and  $d = 3 - 2\epsilon$ . The convenience of dimensional regularization is that it automatically sets power divergences to zero and logarithmic divergences show up as poles in  $\epsilon$ . We define the integrals for integers  $n \geq 0$  as

$$I_n(m^2) = \int_P \frac{1}{(P^2 + m^2)^n}, \quad (59)$$

$$I'_0(m^2) = - \int_P \log [P^2 + m^2], \quad (60)$$

where the prime denotes differentiation with respect to the index  $n$  evaluated at  $n = 0$ . They satisfy the relations

$$\frac{dI'_0(m^2)}{dm^2} = -I_1(m^2), \quad (61)$$

$$\frac{dI_n(m^2)}{dm^2} = -nI_{n+1}(m^2), \quad (62)$$

which follows directly from the definitions Eqs. (59)–(60). The expression for  $I_n(m^2)$  is

$$I_n(m^2) = \frac{m^{4-2n}}{(4\pi)^{\frac{d+1}{2}}} \left( \frac{\Lambda}{m} \right)^{2\epsilon} \frac{\Gamma(n - \frac{d+1}{2})}{\Gamma(n)}. \quad (63)$$

The integrals  $I_n(m^2)$  are divergent for  $n = 1$  and  $n = 2$ . We need the following one-loop integrals expanded to the appropriate order in  $\epsilon$

$$I'_0(m^2) = \frac{m^4}{2(4\pi)^2} \left( \frac{\Lambda'}{m} \right)^{2\epsilon} \left[ \frac{1}{\epsilon} + \frac{3}{2} + \mathcal{O}(\epsilon) \right], \quad (64)$$

$$I_1(m^2) = -\frac{m^2}{(4\pi)^2} \left( \frac{\Lambda'}{m} \right)^{2\epsilon} \left[ \frac{1}{\epsilon} + 1 + \frac{\pi^2 + 12}{12} \epsilon + \mathcal{O}(\epsilon^2) \right], \quad (65)$$

$$I_2(m^2) = \frac{1}{(4\pi)^2} \left( \frac{\Lambda'}{m} \right)^{2\epsilon} \left[ \frac{1}{\epsilon} + \mathcal{O}(\epsilon) \right], \quad (66)$$

where  $\Lambda' = \Lambda(c^2 e)^{\frac{1}{2}}$ . The expression for the setting sun diagram is

$$J(m^2) = \int_{PQ} \frac{p_0^2}{P^2(Q^2 + m^2)[(P+Q)^2 + m^2]} . \quad (67)$$

Generally, for different nonzero masses, the expression for the setting sun diagram is complicated. In the present case with one massless and two equal masses, it simplifies significantly. Using Feynman parameters and averaging over angles, it can be written as a product of two  $I_1(m^2)$  as

$$J(m^2) = \frac{1}{d+1} I_1^2(m^2) . \quad (68)$$

### III. THERMODYNAMIC POTENTIAL AND THERMODYNAMIC QUANTITIES

The thermodynamic potential  $\Omega$  is the object of interest since we can calculate quantities such as the pressure, charge densities, and energy density from it. The thermodynamic potential typically depends on particle masses  $m_i$ , one or more chemical potentials  $\mu_i$  as well as other parameters that we denote by  $\alpha_i$ . We have seen that for zero baryon chemical potential, we have two independent chemical potentials e.g.  $\mu_I$  and  $\mu_S$ . However, the phases we discuss in this paper are always described in terms of a single chemical potential, either  $\mu_I$  or  $\pm\frac{1}{2}\mu_I + \mu_S$ . Similarly, the thermodynamic potential depends on a single additional parameter  $\alpha$ , which in QCD can be identified with the rotation angle of the vacuum (see Sec. IV) and is nonzero in the Bose-condensed phases. When we discuss the weakly interacting Bose gas, the parameter is denoted by  $v$ , which is the condensate density. In the following we therefore write  $\Omega(\mu, \alpha)$ .

The thermodynamic potential can be written as a low-energy expansion in  $\chi$ PT or as an expansion in powers of the dimensionless gas parameter  $\sqrt{na^3}$  in the case of a dilute Bose gas (See Sec. IX A). Thus we write

$$\Omega(\mu, \alpha) = \Omega_0(\mu, \alpha) + \Omega_1(\mu, \alpha) + \dots + \Omega_m(\mu, \alpha) + \dots \quad (69)$$

where the subscript  $m$  denotes the  $m$ th-order contribution in the series. The value of  $\alpha$  that extremizes the thermodynamic potential for a given  $\mu$  is found by solving the equation

$$\frac{\partial \Omega(\mu, \alpha)}{\partial \alpha} = 0 , \quad (70)$$

and is denoted by  $\alpha^*$ . The pressure  $\mathcal{P}$  is equal to minus the thermodynamic potential evaluated  $\alpha = \alpha^*$ , i.e.

$$\mathcal{P}(\mu) = -\Omega(\mu, \alpha^*) . \quad (71)$$

The charge density  $n$  associated with the chemical potential  $\mu$  is

$$n(\mu) = -\left. \frac{\partial \Omega(\mu, \alpha)}{\partial \mu} \right|_{\alpha=\alpha^*} . \quad (72)$$

On the other hand, the pressure  $\mathcal{P}$  is a function of  $\mu$  alone,  $\mathcal{P}(\mu) = -\Omega(\mu, \alpha^*(\mu))$ . This yields

$$\frac{d\mathcal{P}}{d\mu} = -\left[ \frac{\partial \Omega}{\partial \mu} + \frac{\partial \Omega}{\partial \alpha^*} \frac{\partial \alpha^*}{\partial \mu} \right] . \quad (73)$$

Since  $\frac{\partial \Omega}{\partial \alpha^*} = \frac{\partial \Omega}{\partial \alpha} \Big|_{\alpha=\alpha^*}$ , the second term in Eq. (73) vanishes, implying that

$$n(\mu) = \frac{d\mathcal{P}}{d\mu} . \quad (74)$$

Finally, the energy density  $\mathcal{E}(n)$  is given by a Legendre transform of the pressure

$$\mathcal{E}(n) = -\mathcal{P}(\mu) + n(\mu)\mu . \quad (75)$$

The solution  $\alpha^*$  to Eq. (70) can also be written as a series

$$\alpha^* = \alpha_0 + \alpha_1 + \dots , \quad (76)$$

where  $\alpha_0$  is the LO solution. Expanding  $\Omega(\mu, \alpha^*)$  around  $\alpha_0$ , we obtain

$$\begin{aligned} \mathcal{P}(\mu) &= -\Omega(\mu, \alpha^*) = -\Omega_0(\mu, \alpha_0) - \left. \frac{\partial \Omega_0(\mu, \alpha)}{\partial \alpha} \right|_{\alpha=\alpha_0} \alpha_1 \\ &\quad - \Omega_1(\mu, \alpha_0) + \dots \\ &= -\Omega_0(\mu, \alpha_0) - \Omega_1(\mu, \alpha_0) + \dots , \end{aligned} \quad (77)$$

where we have used that the last term in the first line vanishes, cf. Eq. (70). To NLO in the expansion, the pressure is given by the NLO expression for the thermodynamic potential evaluated at the LO minimum  $\alpha_0$ . For completeness, we show how to obtain the first correction  $\alpha_1$ . Eq. (70) is expanded as

$$\begin{aligned} 0 &= \left. \frac{\partial \Omega(\mu, \alpha)}{\partial \alpha} \right|_{\alpha=\alpha^*} \\ &= \left. \frac{\partial \Omega_0(\mu, \alpha)}{\partial \alpha} \right|_{\alpha=\alpha_0} + \left. \frac{\partial^2 \Omega_0(\mu, \alpha)}{\partial \alpha^2} \right|_{\alpha=\alpha_0} \alpha_1 \\ &\quad + \left. \frac{\partial \Omega_1(\mu, \alpha)}{\partial \alpha} \right|_{\alpha=\alpha_0} + \dots . \end{aligned} \quad (78)$$

Since the first term in the second line of Eq. (78) vanishes, we can easily find the first correction to  $\alpha_0$ ,

$$\alpha_1 = -\left. \frac{\partial \Omega_1(\mu, \alpha)}{\partial \alpha} \right|_{\alpha=\alpha_0} \Big/ \left. \frac{\partial^2 \Omega_0(\mu, \alpha)}{\partial \alpha^2} \right|_{\alpha=\alpha_0} . \quad (79)$$

### IV. GROUND STATE AND FLUCTUATIONS AT FINITE DENSITY

In this section, we discuss the form of the ground state and the parametrization of the fluctuations around the ground-state configuration. This discussion has appeared in the literature before, see for example Ref. [12], but we include it here for completeness.

### A. Form of the ground state

We first consider two flavors. The QCD vacuum state is  $\Sigma_0 = \mathbb{1}$ . In order to determine the ground state at finite isospin, we consider the most general SU(2) matrix with constant fields. Using Eq. 1, we can introduce a real parameter  $\alpha$  and constant fields  $\hat{\phi}_a$  via  $\alpha\hat{\phi}_a = \phi_a/f$ , which satisfy  $\hat{\phi}_a\hat{\phi}_a = 1$ . The most general SU(2) matrix can then be parametrized as

$$\Sigma_\alpha = e^{i\hat{\phi}_a\tau_a\alpha}. \quad (80)$$

The subscript  $\alpha$  indicates that this parameter characterizes the ground state, which we will show below. Expanding the exponential and using that the Pauli matrices anticommute, Eq. (80) can be written as

$$\Sigma_\alpha = \mathbb{1} \cos \alpha + i\hat{\phi}_a\tau_a \sin \alpha. \quad (81)$$

The form of the ground state is determined by minimizing the classical thermodynamic potential  $\Omega_0$  as a function of  $\hat{\phi}_a$  and  $\alpha$ , or equivalently by minimizing the static Hamiltonian. The static Hamiltonian is given by  $-\mathcal{L}$  evaluated for constant fields. The first term in the Lagrangian Eq. (24) yields the contribution denoted by  $\Omega_0^{(1)}(\mu_I, \alpha)$  to the thermodynamic potential<sup>5</sup>

$$\begin{aligned} \Omega_0^{(1)}(\mu_I, \alpha) &= \frac{1}{4}f^2\langle[v_0, \Sigma^\dagger][v_0, \Sigma]\rangle \\ &= -\frac{1}{2}f^2\mu_I^2(\hat{\phi}_1^2 + \hat{\phi}_2^2)\sin^2\alpha. \end{aligned} \quad (82)$$

We note that this term only depends on the sum of the squares of  $\hat{\phi}_1$  and  $\hat{\phi}_2$  and is minimized when  $\hat{\phi}_1^2 + \hat{\phi}_2^2$  is as large as possible, i.e. when  $\hat{\phi}_3$  as small as possible due to the constraint  $\hat{\phi}_a\hat{\phi}_a = 1$ . The second term reads

$$\begin{aligned} \Omega_0^{(2)}(\mu_I, \alpha) &= -\frac{1}{4}f^2\langle\chi^\dagger\Sigma + \Sigma^\dagger\chi\rangle \\ &= -f^2B_0(m_u + m_d)\cos\alpha. \end{aligned} \quad (83)$$

Eq. (83) is independent of  $\hat{\phi}_a$ . This implies that the thermodynamic potential is minimized for  $\hat{\phi}_1^2 + \hat{\phi}_2^2 = 1$ . We now see the competition between the two terms in the Lagrangian: The first term prefers  $\sin\alpha$  as large as possible, and the second term prefers  $\cos\alpha$  as large as possible. Writing  $\hat{\phi}_1 = \cos\beta$  and  $\hat{\phi}_2 = \sin\beta$ , we note that the thermodynamic potential is independent of  $\beta$ .  $\Omega_0(\mu_I, \alpha)$  therefore has a flat direction. We can choose this parameter freely and in the remainder we take  $\beta = \frac{1}{2}\pi$ . The ground state can then be written as

$$\Sigma_\alpha = e^{i\tau_2\alpha} = \mathbb{1} \cos \alpha + i\tau_2 \sin \alpha. \quad (84)$$

The state Eq. (84) is a rotation of the quark condensate into a pion condensate by an angle  $\alpha$ , which characterizes the ground state.

The value of  $\alpha$  as a function of  $\mu_I$  is now determined by minimizing the leading-order thermodynamic potential

$$\Omega_0(\mu_I, \alpha) = -f^2m_{\pi,0}^2 \cos \alpha - \frac{1}{2}f^2\mu_I^2 \sin^2 \alpha, \quad (85)$$

where  $m_{\pi,0}^2 = B_0(m_u + m_d)$  is the physical mass of the charged pion at tree level (which is degenerate with the neutral pion since we have not included electromagnetic interactions yet, see section V). The solution  $\alpha_0$  as a function of  $\mu_I$  satisfies

$$\cos \alpha_0 = \begin{cases} 1, & \mu_I^2 \leq m_{\pi,0}^2, \\ \frac{m_{\pi,0}^2}{\mu_I^2}, & \mu_I^2 \geq m_{\pi,0}^2. \end{cases} \quad (86)$$

We next discuss the parameterization of the ground state in the three-flavor case. The most general SU(3) matrix reads

$$\Sigma_\alpha = e^{i\hat{\phi}_a\lambda_a\alpha}. \quad (87)$$

However, since the Gell-Mann matrices do not anticommute, we can not rewrite an SU(3) in a convenient form as in the two-flavor case, Eq. (81). We can nevertheless use our experience in the SU(2) case to write down the form of the ground state. The hint comes from the three SU(2) subgroups of SU(3) generated by  $\{\lambda_1, \lambda_2, \lambda_3\}$ ,  $\{\lambda_4, \lambda_5, \frac{1}{2}(\lambda_3 + \sqrt{3}\lambda_8)\}$ , and  $\{\lambda_6, \lambda_7, \frac{1}{2}(\lambda_3 - \sqrt{3}\lambda_8)\}$  as well as their associated chemical potentials  $\mu_I, \mu_{K^\pm}$ , and  $\mu_{K^0}$ . Pion condensation involves the first SU(2) subgroup, cf. the Pauli matrices  $\tau_a$ . Using the same arguments as above, the ground state can be written as

$$\Sigma_\alpha^{\pi^\pm} = e^{i\lambda_2\alpha} = \frac{1 + 2\cos\alpha}{3}\mathbb{1} + \frac{\cos\alpha - 1}{\sqrt{3}}\lambda_8 + i\lambda_2 \sin\alpha, \quad (88)$$

where the superscript indicates the condensing mode. Note that, even though this state is written in terms of  $\lambda_8$ , which is not a generator of the first SU(2) subgroup, this is still an element of that group. The ground state commutes with  $\lambda_3$  only for  $\alpha = 0$ . This means that the  $U(1)_{I_3}$  symmetry is spontaneously broken in the pion-condensed phase, which by Goldstone's theorem leads to a massless excitation. Since the quark charge matrix can be written as  $\frac{1}{2}(\lambda_3 + \frac{\lambda_8}{\sqrt{3}})$ , the symmetry generated by the electric charge  $Q$  is also broken in this phase. In the presence of dynamical photons, this phase is a superconducting Higgs phase with a massive photon. This will be discussed in section V.

Similar arguments apply in the remaining cases of charged and neutral kaon condensation, as the corresponding chemical potential appears together with the generators of the remaining two SU(2) subgroups. The

<sup>5</sup> In the two-flavor case,  $v_0 = \frac{1}{3}\mu_B\mathbb{1} + \frac{1}{2}\mu_I\tau_3$ , cf. Eq. (10).



ground states are parametrized as

$$\begin{aligned} \Sigma_\alpha^{K^\pm} &= e^{i\lambda_5\alpha} = \frac{1+2\cos\alpha}{3}\mathbb{1} + \frac{\cos\alpha-1}{2\sqrt{3}}\left(\sqrt{3}\lambda_3 - \lambda_8\right) \\ &\quad + i\lambda_5\sin\alpha, \end{aligned} \quad (89)$$

$$\begin{aligned} \Sigma_\alpha^{K^0/\bar{K}^0} &= e^{i\lambda_7\alpha} = \frac{1+2\cos\alpha}{3}\mathbb{1} + \frac{1-\cos\alpha}{2\sqrt{3}}\left(\sqrt{3}\lambda_3 + \lambda_8\right) \\ &\quad + i\lambda_7\sin\alpha. \end{aligned} \quad (90)$$

In the case of neutral kaon condensation, the phase is a superfluid, but not a superconductor. In the next section, we will use the expressions for the ground states to calculate the pressure and other thermodynamic quantities to leading order in the low-energy expansion.

The form of our parametrization in the three-flavor case is based on our experience with the two-flavor case. For given values of  $\mu_I$  and  $\mu_S$ , we have four candidates for the ground state, namely the vacuum and the three states in Eqs. (88)–(90). For each of the three states, we minimize the thermodynamic potential. We compare the pressure of the four candidates and the state with the highest pressure is our ground state. Strictly speaking, we have not shown that our ground state corresponds to a minimum of the tree-level potential. Expanding in fluctuations about this point, it turns out that the linear terms vanish (see Subsec. IV B) and that the masses are real (see Subsec. V B). Thus it is locally stable, i.e. at least a metastable point. We will simply assume that it is also the global minimum.

Let us finally comment on the order of the transitions from the vacuum to a Bose-condensed phase. The Bose condensate is an order parameter and in order to calculate it, we need to couple the system to an external pionic source  $j$ , cf Eq. (7). In the case of pion condensation, the external field becomes

$$\chi = 2B_0M + 2iB_0\lambda_2j. \quad (91)$$

The leading-order thermodynamic potential then reads

$$\begin{aligned} \Omega_0(\mu_I, \alpha) &= -f^2B_0(m_u + m_d)\cos\alpha - f^2B_0m_s \\ &\quad - 2f^2B_0j\sin\alpha - \frac{1}{2}f^2\mu_I^2\sin^2\alpha. \end{aligned} \quad (92)$$

The quark and pion condensates are then given by the derivatives of  $\Omega(\mu_I, \alpha)$  with respect to  $m_{u,d}$  and  $j$  as

$$\begin{aligned} \langle \bar{q}q \rangle &= \frac{\partial\Omega_0(\mu_I, \alpha)}{\partial m_u} + \frac{\partial\Omega_0(\mu_I, \alpha)}{\partial m_d} \\ &= -2f^2B_0\cos\alpha = \langle \bar{q}q \rangle_{\text{vac}}\cos\alpha, \end{aligned} \quad (93)$$

$$\begin{aligned} \langle \bar{q}\gamma^5 i\lambda_2q \rangle &= \frac{\partial\Omega_0(\mu_I, \alpha)}{\partial j} \\ &= -2f^2B_0\sin\alpha = \langle \bar{q}q \rangle_{\text{vac}}\sin\alpha, \end{aligned} \quad (94)$$

where  $\langle \bar{q}q \rangle_{\text{vac}}$  is the vacuum value of the quark condensate. We note that the sum of the square of the condensates is constant and equals the square of the quark condensate in the vacuum. Thus the quark condensate is

rotated into a pion condensate. Using  $\cos\alpha = m_{\pi,0}^2/\mu_I^2$ , we obtain

$$\langle \bar{q}\gamma^5 i\lambda_2q \rangle = \langle \bar{q}q \rangle_{\text{vac}}\sqrt{1 - \frac{m_{\pi,0}^4}{\mu_I^4}}. \quad (95)$$

Close to the phase transition where  $\mu_I \approx m_{\pi,0}$  and  $\mu_I + m_{\pi,0} \approx 2m_{\pi,0}$ , this reduces to

$$\langle \bar{q}\gamma^5 i\lambda_2q \rangle = 2\langle \bar{q}q \rangle_{\text{vac}}\sqrt{1 - \frac{m_{\pi,0}}{\mu_I}}. \quad (96)$$

Thus the order parameter is a continuous function of  $\mu_I$  close to the transition, which therefore is of second order. The mean-field critical exponent is  $\frac{1}{2}$ , which follows directly from Eq. (96) and the system is in the  $O(2)$  universality class.

There is another way to see this, based directly on a Ginzburg-Landau analysis of the thermodynamic potential. Expanding the thermodynamic potential Eq. (85) in powers of  $\alpha$  around  $\alpha = 0$  to order  $\alpha^4$ , we obtain

$$\begin{aligned} \Omega_0(\mu_I, \alpha) &= -f^2m_{\pi,0}^2 + \frac{1}{2}f^2[m_{\pi,0}^2 - \mu_I^2]\alpha^2 \\ &\quad + \frac{1}{24}f^2[4\mu_I^2 - m_{\pi,0}^2]\alpha^4. \end{aligned} \quad (97)$$

A critical isospin chemical potential  $\mu_I^c$  is defined by the vanishing of the quadratic term in the equation above. This yields  $\mu_I^c = \pm m_{\pi,0}$ . Since the quartic term is positive for  $\mu_I = \mu_I^c$ , the transition is second order. The value of  $\alpha$  that minimizes Eq. (97) is

$$\alpha_0 = \sqrt{\frac{6(\mu_I^2 - m_{\pi,0}^2)}{4\mu_I^2 - m_{\pi,0}^2}}. \quad (98)$$

Close to the transition,  $\alpha = 2\sqrt{1 - \frac{m_{\pi,0}}{\mu_I}}$ . The onset of BEC when  $\mu_I$  is equal to the mass of the charged pion at tree level is a leading-order result, but is expected to hold to all orders in the low-energy expansion, where the physical pion mass is calculated in the same approximation as the thermodynamic potential. This was explicitly shown in Ref. [30] to order  $\mathcal{O}(p^4)$ , where  $m_{\pi,0}$  is replaced by its NLO expression, Eq. (236).

## B. Fluctuations

The ground state  $\Sigma_\alpha$  minimizes the energy for given values of  $\mu_I$  and  $\mu_S$ . We would like to include quantum corrections and we therefore need to discuss the parametrization of the fluctuations around the ground state. In the vacuum,  $\alpha = 0$ , we have  $\Sigma = U\Sigma_0U$ , where

$$U = e^{\frac{1}{2}i\phi_a\lambda_a/f}. \quad (99)$$

A naive way of parametrizing  $\Sigma$  for arbitrary  $\alpha$  is

$$\Sigma = U\Sigma_\alpha U. \quad (100)$$

Using this parametrization, one can expand the Lagrangian  $\mathcal{L}_2$  to second order in the fluctuations. It turns out that the kinetic terms are not canonically normalized so one needs a field redefinition, which happens to depend on the chemical potential. After redefining the field one can calculate the NLO contribution to the thermodynamic potential arising from the functional determinant in the standard way. The counterterms, given by the static part of the NLO Lagrangian  $\mathcal{L}_4$ , are already fixed and do not cancel the divergences for arbitrary values of  $\alpha$ , only for the value that corresponds to the minimum of the tree-level thermodynamic potential, Eq. (86). In other words, we cannot renormalize the NLO thermodynamic potential away from the classical minimum and therefore not determine the value of  $\alpha$  that minimizes it. The problem is that the parametrization Eq. (100) is not valid for nonzero  $\alpha$ , which was first pointed out in Ref. [12]. Introducing

$$L_\alpha = A_\alpha U A_\alpha^\dagger, \quad R_\alpha = A_\alpha^\dagger U^\dagger A_\alpha, \quad (101)$$

where  $A_\alpha = e^{\frac{1}{2}i\lambda_\alpha}$  (with  $a = 2, 5, 7$  depending on the ground state we consider), the correct parametrization is

$$\Sigma = L_\alpha \Sigma_\alpha R_\alpha^\dagger = A_\alpha (U \Sigma_0 U) A_\alpha. \quad (102)$$

Using this parametrization, the kinetic terms are automatically canonically normalized. Moreover, the  $\mathcal{O}(p^4)$  counterterms cancel the ultraviolet divergences arising from the functional determinant for all values of  $\alpha$ , as we shall see in section VI.

Using the parametrization Eq. (102) in the Lagrangian (24) and expanding in powers of the fields, we obtain  $\mathcal{L}_2 = \mathcal{L}_2^{(0)} + \mathcal{L}_2^{(1)} + \dots$ , where the superscript indicates the order in the fields. To be specific, we consider pion condensation. The zeroth-order term is  $\mathcal{L}_2^{(0)} = -\Omega_0(\mu_I, \alpha)$ , from the previous section. The linear term is

$$\mathcal{L}_2^{(1)} = f [(\mu_I^2 \cos \alpha - m_{\pi,0}^2) \phi_2 - \mu_I \partial_0 \phi_1] \sin \alpha \quad (103)$$

The  $\partial_0 \phi_1$  term is a total derivative and can therefore be ignored. The remaining terms vanish for  $\alpha = 0$  or  $\cos \alpha = m_{\pi,0}^2 / \mu_I^2$ , which exactly is the value of  $\alpha$  that minimizes  $\Omega_0(\mu_I, \alpha)$ . In the next section, we calculate the masses showing that the point we expand about is a minimum. We can draw similar conclusions for the charged and neutral kaon condensates. For a given pair of  $\mu_I$  and  $\mu_S$ , we calculate the energy of the ground state of different phases and determine which is the global minimum and in this manner map out the phase diagram. This is also done in the next section.

We close this section with a few remarks on finite density and symmetry breaking. The conventional view is that the introduction of a chemical potential  $\mu$  breaks Lorentz invariance explicitly. However, in recent years an alternative view has been put forward by Nicolis and collaborators [64, 65], namely that Lorentz invariance is

broken spontaneously. At finite chemical potential  $\mu$ , one uses the grand-canonical Hamiltonian defined as

$$\mathcal{H}' = \mathcal{H} - \mu Q, \quad (104)$$

where  $\mathcal{H}$  is the original Hamiltonian of the system and  $Q$  is the conserved charge that is a consequence of a continuous symmetry via Noether's theorem and associated with  $\mu$ . We are interested in the ground state  $|\mu\rangle$  of the modified Hamiltonian  $\mathcal{H}'$ , satisfying

$$\mathcal{H}'|\mu\rangle = 0. \quad (105)$$

The right-hand side should read  $\lambda|\mu\rangle$ , but  $\lambda$  can always be set to zero via a redefinition of the cosmological constant [64]. If the charge  $Q$  is spontaneously broken, it follows from Eq. (105) that time translations (which are generated by  $\mathcal{H}$ ) are also spontaneously broken since the state  $|\mu\rangle$  is not an eigenstate of the original Hamiltonian  $\mathcal{H}$ . However, spatial translations are not broken, which singles out the time direction as being special. The fact that spatial translational symmetries are intact implies that the state  $|\mu\rangle$  breaks all Lorentz boosts. On the other hand, a new time translation symmetry is unbroken, namely the translations generated by  $\mathcal{H}' = \mathcal{H} - \mu Q$ . Summarizing, all the Lorentz boosts and the internal symmetry generated by  $Q$  are all spontaneously broken, while translations (space and time), rotations and the internal symmetries not generated by  $Q$  remain unbroken. In the case of pion condensation,  $Q = Q_{I_3}$  is the third component of the isospin and the internal symmetry that is broken spontaneously by the Bose condensate is  $U(1)_{I_3}$ .

The idea is that instead of doing perturbation theory around a time-independent ground state, one expands around a time-dependent ground state. We have denoted the time-independent ground state by  $\Sigma_\alpha^{\pi^\pm}$ . Similarly, we denote the time-dependent ground state by  $\Sigma_\alpha^{\pi^\pm}(t)$ , this state can be written as

$$\begin{aligned} \Sigma_\alpha^{\pi^\pm}(t) &= e^{-\frac{1}{2}i\lambda_3\mu_I t} \Sigma_\alpha^{\pi^\pm} e^{\frac{1}{2}i\lambda_3\mu_I t} \\ &= e^{-\frac{1}{2}i\lambda_3\mu_I t} A_\alpha \Sigma_0 A_\alpha e^{\frac{1}{2}i\lambda_3\mu_I t}. \end{aligned} \quad (106)$$

The ground state Eq. (106) breaks time invariance, hence it is broken spontaneously. Perturbation theory is now carried out around this state with the original chiral Lagrangian with  $\mu_I = 0$ , which is Lorentz invariant. This can be seen as follows. The field, now denoted by  $\tilde{\Sigma}$ , is parametrized as

$$\begin{aligned} \tilde{\Sigma} &= e^{-\frac{1}{2}i\lambda_3\mu_I t} \Sigma e^{\frac{1}{2}i\lambda_3\mu_I t} \\ &= e^{-\frac{1}{2}i\lambda_3\mu_I t} A_\alpha U \Sigma_0 U A_\alpha e^{\frac{1}{2}i\lambda_3\mu_I t}. \end{aligned} \quad (107)$$

It can then be shown that

$$\partial_\mu \tilde{\Sigma} = e^{-\frac{1}{2}i\lambda_3\mu_I t} (\nabla_\mu \Sigma) e^{\frac{1}{2}i\lambda_3\mu_I t}, \quad (108)$$

$$\tilde{\Sigma} \chi^\dagger = e^{-\frac{1}{2}i\lambda_3\mu_I t} \Sigma \chi^\dagger e^{\frac{1}{2}i\lambda_3\mu_I t}, \quad (109)$$

where we have used that  $\lambda_3$  and the quark mass matrix commute. Using  $\partial_\mu \tilde{\Sigma}$ ,  $\tilde{\Sigma} \chi^\dagger$  as well as their Hermitian conjugates as building blocks, together with the cyclicity of the trace, we recover the original Lagrangian.

## V. LEADING-ORDER RESULTS

In this section, we derive some leading-order results, namely the quasiparticle masses in the pion-condensed phase, pressure, densities (isospin and strangeness), and the phase diagram in the  $\mu_I$ - $\mu_S$  plane. However, before these results are presented, we discuss how the parameters in the chiral Lagrangian are related to physical observables.

### A. Parameter fixing

In order to find the tree-level masses, we expand the LO chiral Lagrangian to second order in the fields,

$$\begin{aligned} \mathcal{L}_2^{(2)} = & -\frac{1}{4}F_{\mu\nu}F^{\mu\nu} + \frac{1}{2}\partial_\mu\phi_a\partial^\mu\phi_a - \frac{1}{2}m_a^2\phi_a^2 \\ & + \frac{1}{\sqrt{3}}\Delta m^2\phi_3\phi_8 + \partial_\mu\bar{c}\partial^\mu c - \frac{1}{2\xi}(\partial_\mu A^\mu)^2 \end{aligned} \quad (110)$$

Here the masses are

$$m_1^2 = B_0(m_u + m_d) + \Delta m_{\text{EM}}^2 = m_{\pi,0}^2 + \Delta m_{\text{EM}}^2 \quad (111)$$

$$m_2^2 = B_0(m_u + m_d) + \Delta m_{\text{EM}}^2 = m_{\pi,0}^2 + \Delta m_{\text{EM}}^2 \quad (112)$$

$$m_3^2 = B_0(m_u + m_d) = m_{\pi,0}^2, \quad (113)$$

$$m_4^2 = B_0(m_u + m_s) + \Delta m_{\text{EM}}^2 = m_{K^\pm,0}^2 + \Delta m_{\text{EM}}^2 \quad (114)$$

$$m_5^2 = B_0(m_u + m_s) + \Delta m_{\text{EM}}^2 = m_{K^\pm,0}^2 + \Delta m_{\text{EM}}^2 \quad (115)$$

$$m_6^2 = B_0(m_d + m_s) = m_{K^0,0}^2, \quad (116)$$

$$m_7^2 = B_0(m_d + m_s) = m_{K^0,0}^2, \quad (117)$$

$$m_8^2 = \frac{1}{3}B_0(m_u + m_d + 4m_s) = m_{\eta,0}^2, \quad (118)$$

with

$$\Delta m^2 = B_0(m_d - m_u), \quad (119)$$

$$\Delta m_{\text{EM}}^2 = \frac{2Ce^2}{f^2}. \quad (120)$$

The photon as well as the massless ghost field decouple in the vacuum phase so we do not discuss them any further. Moreover, away from the isospin limit, the off-diagonal terms in Eq. (110) lead to mixing. The vacuum masses are given by the poles of the propagator

$$\begin{aligned} m_{\pi^0/\eta^0}^2 = & \frac{1}{3} \left( m_{K^\pm,0}^2 + m_{K^0,0}^2 + m_{\pi,0}^2 \right. \\ & \left. \mp \sqrt{(m_{K^\pm,0}^2 + m_{K^0,0}^2 - 2m_{\pi,0}^2)^2 + 3(\Delta m^2)^2} \right), \end{aligned} \quad (121)$$

$$m_{\pi^\pm}^2 = m_{\pi,0}^2 + \Delta m_{\text{EM}}^2, \quad (122)$$

$$m_{K^0}^2 = m_{K^\pm,0}^2 + \Delta m^2, \quad (123)$$

$$m_{K^\pm}^2 = m_{K^\pm,0}^2 + \Delta m_{\text{EM}}^2. \quad (124)$$

The mass splittings between neutral and charge mesons have two sources. The first arises from the electromagnetic interactions,  $\Delta m_{\text{EM}}^2 = \frac{2Ce^2}{f^2}$ , which is the same for pions and kaons. This is Dashen's theorem [49]. The second source of mass splitting is the mass difference between the  $u$  and the  $d$  quark, encoded in  $\Delta m^2$ . For the pion this takes a more complicated form, due to the mixing of  $\pi^0$  and  $\eta$ . To leading order in  $\Delta m^2$ , Eq. (121) yields

$$m_{\pi^0}^2 = m_{\pi,0}^2 - \frac{1}{4} \frac{(\Delta m^2)^2}{m_{K^\pm,0}^2 - m_{\pi,0}^2}. \quad (125)$$

Therefore,  $m_{\pi^\pm}^2 = m_{\pi,0}^2 + \Delta m_{\text{EM}}^2 + \mathcal{O}((\Delta m^2)^2)$ , and the mass splitting is dominated by the electromagnetic contribution. For the kaon, on the other hand, the contributions are of the same order,

$$m_{K^\pm}^2 = m_{K^0}^2 - \Delta m^2 + \Delta m_{\text{EM}}^2, \quad (126)$$

Notice that the corrections pull in opposite directions, decreasing the absolute value of the mass splitting.

The meson masses given above in Eqs. (121)–(124) are the poles masses at tree level. The measured values of the meson masses are taken from the Particle Data Group [66],

$$m_{\pi^0} = 134.98 \text{ MeV}, \quad m_{\pi^\pm} = 139.57 \text{ MeV}, \quad (127)$$

$$m_{K^\pm} = 493.68 \text{ MeV}, \quad m_{K^0} = 497.61 \text{ MeV}. \quad (128)$$

Solving Eqs. (121)–(124) numerically with the experimental values given above, we obtain

$$m_{\pi,0} = 135.09 \text{ MeV}, \quad m_{K^\pm,0} = 492.43 \text{ MeV}, \quad (129)$$

$$\Delta m^2 = (71.60 \text{ MeV})^2, \quad \Delta m_{\text{EM}}^2 = (35.09 \text{ MeV})^2. \quad (130)$$

Using the values for the pion masses above and the decay constant and electromagnetic coupling from [66],

$$f_\pi = 92.07 \text{ MeV}, \quad e = 0.3028, \quad (131)$$

we find that the coupling  $C$  introduced in Ref. [47] is

$$C = \frac{f^2}{2e^2} \Delta m_{\text{EM}}^2 = 5.692 \times 10^{-5} (\text{GeV})^4, \quad (132)$$

where we have used that  $f = f_\pi$  at tree level. We note in passing that the constant  $C$  can be expressed in terms of the mass of the  $\rho$  meson, its decay constant  $f_\rho$ , and  $f_\pi$  as [67]

$$C = \frac{3m_\rho^2 f_\rho^2}{2(4\pi)^2} \ln \left( \frac{f_\rho^2}{f_\rho^2 - f_\pi^2} \right). \quad (133)$$

Using the values  $f_\pi = 93.3 \text{ MeV}$ ,  $f_\rho = 154 \text{ MeV}$  and  $m_\rho = 770 \text{ MeV}$ , Urech [48] obtains the numerical value  $6.11 \times 10^{-5} (\text{GeV})^4$ .

## B. Quasiparticle masses

In order to calculate the quasiparticles masses, we expand the LO chiral Lagrangian to the second order in the fields. We do this in the pion-condensed phase, similar results can be obtained for the kaon-condensed phases. For simplicity, we consider  $\mu_S = 0$ . The quadratic terms are

$$\begin{aligned} \mathcal{L}_2^{(2)} = & -\frac{1}{4}F_{\mu\nu}F^{\mu\nu} + \frac{1}{2}m_A^2\eta_{\mu\nu}A^\mu A^\nu + \frac{1}{2}\partial_\mu\phi_a\partial^\mu\phi_a \\ & + \frac{1}{2}m_{ab}\phi_a\partial_0\phi_b - m_{\phi A}^2\phi_2A^0 - \frac{1}{2}m_a^2\phi_a^2 \\ & - ef\sin\alpha\partial_\mu A^\mu\phi_1 + \frac{1}{\sqrt{3}}\Delta m^2\phi_3\phi_8 + \partial_\mu\bar{c}\partial^\mu c \\ & - m_c^2\bar{c}c - \frac{1}{2\xi}(\partial_\mu A^\mu)^2, \end{aligned} \quad (134)$$

where the diagonal mass terms are

$$m_1^2 = m_{\pi,0}^2 \cos\alpha - (\mu_I^2 - \Delta m_{\text{EM}}^2) \cos^2\alpha + \xi e^2 f^2 \sin^2\alpha, \quad (135)$$

$$m_2^2 = m_{\pi,0}^2 \cos\alpha - (\mu_I^2 - \Delta m_{\text{EM}}^2) \cos 2\alpha, \quad (136)$$

$$m_3^2 = m_{\pi,0}^2 \cos\alpha + (\mu_I^2 - \Delta m_{\text{EM}}^2) \sin^2\alpha, \quad (137)$$

$$\begin{aligned} m_4^2 = & m_{K^\pm,0}^2 + \frac{1}{2}m_{\pi,0}^2(\cos\alpha - 1) - \frac{1}{4}\mu_I^2 \cos 2\alpha \\ & + \frac{1}{2}\Delta m_{\text{EM}}^2 \cos\alpha(\cos\alpha + 1), \end{aligned} \quad (138)$$

$$\begin{aligned} m_6^2 = & m_{K^0,0}^2 + \frac{1}{2}m_{\pi,0}^2(\cos\alpha - 1) - \frac{1}{4}\mu_I^2 \cos 2\alpha \\ & + \frac{1}{2}\Delta m_{\text{EM}}^2 \cos\alpha(\cos\alpha - 1), \end{aligned} \quad (139)$$

$$m_8^2 = m_{\eta,0}^2 + \frac{1}{3}m_{\pi,0}^2(\cos\alpha - 1), \quad (140)$$

$$m_A^2 = e^2 f^2 \sin^2\alpha, \quad (141)$$

$$m_c^2 = \xi e^2 f^2 \sin^2\alpha, \quad (142)$$

with  $m_6^2 = m_7^2$  and  $m_4^2 = m_5^2$ . The nonvanishing off-diagonal terms are

$$m_{12} = 2\mu_I \cos\alpha, \quad (143)$$

$$m_{45} = \mu_I \cos\alpha, \quad (144)$$

$$m_{67} = -\mu_I \cos\alpha, \quad (145)$$

with  $m_{ab} = -m_{ba}$ . The coupling between  $\phi_2$  and  $A^0$  is given by

$$m_{\phi A}^2 = ef\mu_I \sin 2\alpha. \quad (146)$$

The spectra of the mesons are

$$\begin{aligned} E_{\pi^0/\eta}^2 = & p^2 + \frac{1}{2}(m_3^2 + m_8^2) \\ & \mp \frac{1}{2\sqrt{3}}\sqrt{3(m_3^2 - m_8^2)^2 + 4(\Delta m^2)^2}, \end{aligned} \quad (147)$$

$$\begin{aligned} E_{\tilde{\pi}^\pm}^2 = & p^2 + \frac{1}{2}(m_1^2 + m_2^2 + m_{12}^2) \\ & \mp \frac{1}{2}\sqrt{4p^2 m_{12}^2 + (m_1^2 + m_2^2 + m_{12}^2)^2 - 4m_1^2 m_2^2}, \end{aligned} \quad (148)$$

$$E_{K^\pm}^2 = p^2 + m_4^2 + \frac{1}{2}m_{45}^2 \mp \frac{1}{2}m_{45}\sqrt{4p^2 + 4m_4^2 + m_{45}^2}, \quad (149)$$

$$E_{\bar{K}^0/\bar{K}^0}^2 = p^2 + m_6^2 + \frac{1}{2}m_{67}^2 \pm \frac{1}{2}m_{67}\sqrt{4p^2 + 4m_6^2 + m_{67}^2}. \quad (150)$$

The modes in Eq. (147) are identified with the neutral pion and the  $\eta$ . The modes in Eq. (148) are linear combinations of  $\pi^+$  and  $\pi^-$ , denoted by a  $\tilde{\pi}^\pm$ . At onset of pion condensation,  $\tilde{\pi}^+$  coincides with  $\pi^+$  and  $\tilde{\pi}^-$  coincides with  $\pi^-$ . Similar remarks apply to the kaon modes, Eqs. (149) and (150). The effective masses of the particle are then given by  $m = E(p=0)$ . In the remainder, we choose the Feynman gauge,  $\xi = 1$ . The ghost and the photon have the same mass and the ghost interacts with the would-be Goldstone, cf. Eq. (26). The cross term in the gauge-fixing Lagrangian cancels the term  $-ef\sin\alpha\partial^\mu A_\mu\phi_1$  in Eq. (134). There are still two mixing terms, namely between  $\phi_3$  and  $\phi_8$ , and between  $\phi_2$  and  $A^0$ , making the inverse propagator matrix rather complicated. Due to this, the long expressions for the dispersion relations will be not listed, only the quasiparticle masses will be given. In the symmetric phase,  $\alpha = 0$ , the mixing between  $\phi_2$  and  $A^0$  vanishes and the photon decouples. The ghost and the photon are both massless. The remaining masses in the symmetric phase are

$$m_{\pi^0/\eta}^2 = \frac{1}{3}\left(m_{K^\pm,0}^2 + m_{K^0,0}^2 + m_{\pi,0}^2 \quad (151)\right.$$

$$\left. \mp \sqrt{(m_{K^\pm,0}^2 + m_{K^0,0}^2 - 2m_{\pi,0}^2)^2 + 3(\Delta m^2)^2}\right),$$

$$m_{\tilde{\pi}^\pm}^2 = \left(\sqrt{m_{\pi,0}^2 + \Delta m_{\text{EM}}^2} \mp \mu_I\right)^2, \quad (152)$$

$$m_{K^\pm}^2 = \left(\sqrt{m_{K^\pm,0}^2 + \Delta m_{\text{EM}}^2} \mp \frac{1}{2}\mu_I\right)^2, \quad (153)$$

$$m_{\bar{K}^0/\bar{K}^0}^2 = \left(m_{K^0,0} \mp \frac{1}{2}\mu_I\right)^2. \quad (154)$$

Due to the finite chemical potential  $\mu_I$ , the charged excitations Eqs. (152)–(153) are linear combinations of the corresponding excitations in the vacuum and they are denoted by  $\tilde{\pi}^\pm$  etc.

In the last section, we found that the transition from the vacuum phase to the symmetry-broken phase happens at  $\mu_I^2 = m_{\pi,0}^2$ . When electromagnetic effects

are included, the critical chemical potential is  $\mu_{I,\text{eff}}^2 = \mu_I^2 - \Delta m_{\text{EM}}^2 = m_{\pi,0}^2$  or  $\mu_I^2 = m_{\pi^\pm,0}^2$  (see details in Subsec. VC). In the pion-condensed phase, the U(1) symmetry generated by  $\lambda_3$  is broken and in the absence of electromagnetic effects, a massless excitation appears in the spectrum. The generator of electric charge  $\lambda_Q = \lambda_3 + \frac{1}{\sqrt{3}}\lambda_8$ . Once this symmetry is gauged, it

can no longer be broken (Elitzur's theorem), the Goldstone boson disappears from the spectrum, being "eaten" by the photon via the Higgs mechanism. As a result, the photon becomes massive with three polarization states. At tree level, we have  $\cos \alpha_0 = m_{\pi,0}^2/\mu_{I,\text{eff}}^2 = m_{\pi,0}^2/(\mu_I^2 - \Delta m_{\text{EM}}^2)$ , see Eq. (161) below. Defining  $\tilde{m}^2 = \frac{2}{3}(m_{K^\pm,0}^2 + m_{K^0,0}^2 - m_{\pi,0}^2)$ , the different masses are

$$m_{\pi^0/\eta}^2 = \frac{1}{2}(\tilde{m}^2 + \mu_{I,\text{eff}}^2) + \frac{m_{\pi,0}^4}{6\mu_{I,\text{eff}}^2} \mp \frac{1}{6\mu_{I,\text{eff}}^2} \sqrt{12(\Delta m^2)^2 \mu_{I,\text{eff}}^4 + [3\mu_{I,\text{eff}}^2(\tilde{m}^2 - \mu_{I,\text{eff}}^2) + m_{\pi,0}^4]^2}, \quad (155)$$

$$m_{\bar{K}^0/K^0}^2 = m_{K^0,0}^2 + \frac{1}{4}\mu_I^2 + \frac{m_{\pi,0}^2 \mu_I^2 (m_{\pi,0}^2 - \mu_{I,\text{eff}}^2)}{2\mu_{I,\text{eff}}^4} \mp \frac{m_{\pi,0}^2 |\mu_I|}{2\mu_{I,\text{eff}}^4} \sqrt{\mu_I^2 m_{\pi,0}^4 + \mu_{I,\text{eff}}^2 [\mu_I^2 (\mu_{I,\text{eff}}^2 - 2m_{\pi,0}^2) + 4m_{K^0,0}^2 \mu_{I,\text{eff}}^2]}, \quad (156)$$

$$m_{\bar{K}^\pm}^2 = m_{K^\pm,0}^2 + \frac{1}{4}\mu_I^2 + \frac{m_{\pi,0}^2}{2\mu_{I,\text{eff}}^4} [\mu_I^2 m_{\pi,0}^2 - \mu_{I,\text{eff}}^2 (\mu_{I,\text{eff}}^2 - \Delta m_{\text{EM}}^2)] \mp \frac{m_{\pi,0}^2 |\mu_I|}{2\mu_{I,\text{eff}}^4} \times \sqrt{\mu_I^2 m_{\pi,0}^4 + \mu_{I,\text{eff}}^2 [\mu_I^2 (\mu_{I,\text{eff}}^2 - 2m_{\pi,0}^2) + 4m_{K^\pm,0}^2 \mu_{I,\text{eff}}^2 + 4\Delta m_{\text{EM}}^2 m_{\pi,0}^2]}, \quad (157)$$

$$m_{\pi^-}^2 = \mu_{I,\text{eff}}^2 \left[ 1 + \frac{m_{\pi,0}^4 (3\mu_{I,\text{eff}}^2 + 4\Delta m_{\text{EM}}^2)}{\mu_{I,\text{eff}}^6} \right], \quad (158)$$

$$m_A^2 = e^2 f^2 \left[ 1 - \frac{m_{\pi,0}^2}{\mu_{I,\text{eff}}^2} \right]. \quad (159)$$

In Fig. 3, the masses are plotted as functions of the isospin chemical potential normalized to the mass of the charged pion. We see that the masses are continuous functions of the chemical potential, but they are non-differentiable across the phase transition. Note also that the charged pion vanishes from the spectrum at the critical chemical potential (green line in the lower panel). The photon becomes massive, as explained above.

Fig. 4 shows the behavior of the masses for higher values of the isospin chemical potential. At one point, the mass of the neutral pion and  $\eta$  come close to overlapping. This happens as the second term under the root in Eq. (155) vanishes. If  $\Delta m^2 = 0$ , the root vanishes and the absolute value leads to a non-differentiable behavior as the lines intersect. For  $\Delta m^2 \neq 0$ , the lines are smooth, and there opens up a gap, as indicated in the figure. Above this point, the two masses "change roles", as the neutral pion mass approaches a constant, while the  $\eta$  mass grows linearly.

### C. Thermodynamic quantities and phase diagram

In this section, we calculate the pressure  $\mathcal{P}$  and present the phase diagram at  $T = 0$  in the  $\mu_I - \mu_S$  plane for three-flavor  $\chi$ Pt including electromagnetic effects.

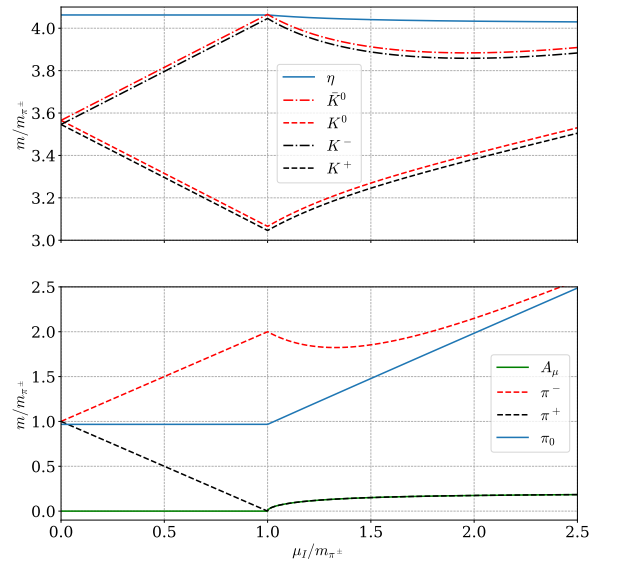


FIG. 3. Quasi-particle masses at leading order in  $\chi$ Pt as functions of the isospin chemical potential  $\mu_I$  normalized to  $m_{\pi^\pm}$ . See main text for details.

The leading-order thermodynamic potential in the pion-

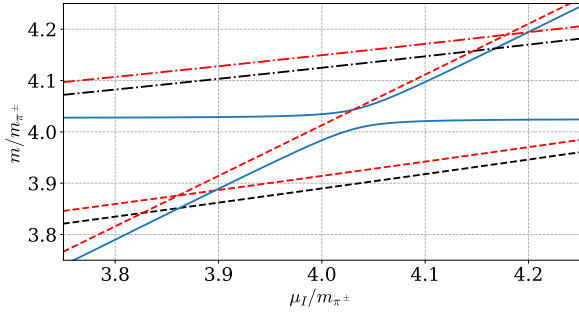


FIG. 4. The masses of the  $\pi^0$  and the  $\eta$  approach each other before “changing roles”, as described in the main text.

condensed phase is

$$\Omega_0(\mu_I, \alpha) = -f^2 \left[ m_{\pi,0}^2 \cos \alpha + B_0 m_s + \frac{1}{3} \Delta m_{\text{EM}}^2 + \frac{1}{2} (\mu_I^2 - \Delta m_{\text{EM}}^2) \sin^2 \alpha \right], \quad (160)$$

where we have used the form of the ground state  $\Sigma_\alpha^{\pi^\pm}$  given in Eq. (88). The value  $\alpha$  that extremizes  $\Omega_0(\mu_I, \alpha)$  satisfies

$$\cos \alpha_0 = \frac{m_{\pi,0}^2}{\mu_I^2 - \Delta m_{\text{EM}}^2} = \frac{m_{\pi,0}^2}{\mu_{I,\text{eff}}^2}, \quad (161)$$

valid for  $\mu_{I,\text{eff}}^2 = \mu_I^2 - \Delta m_{\text{EM}}^2 \geq m_{\pi,0}^2$ . The transition therefore takes place at  $\mu_{I,\text{eff}}^2 = m_{\pi,0}^2$ , which is equivalent to  $\mu_I^2 = m_{\pi^\pm}^2 = m_{\pi,0}^2 + \Delta m_{\text{EM}}^2$ , i.e. the tree-level mass of the charged pion. The pressure is expressed as  $\mathcal{P}(\mu_I) = -\Omega_0(\mu_I, \alpha_0)$ . Subtracting the pressure in the vacuum phase, we obtain

$$\mathcal{P} = \frac{1}{2} f^2 \mu_{I,\text{eff}}^2 \left[ 1 - \frac{m_{\pi,0}^2}{\mu_{I,\text{eff}}^2} \right]^2. \quad (162)$$

In the pion-condensed phase, the isospin and strangeness densities  $n_I$  and  $n_S$  are obtained from  $n = \frac{d\mathcal{P}}{d\mu}$ , which gives

$$n_I = f^2 \mu_I \left[ 1 - \frac{m_{\pi,0}^4}{\mu_{I,\text{eff}}^4} \right], \quad n_S = 0. \quad (163)$$

We note that the leading-order results for the pion-condensed phase, Eqs. (162)–(163), are independent of  $m_s$  and are identical to the results in two-flavor  $\chi$ PT.

The pressure and the densities of the other phases can be calculated in the same way, using the corresponding parametrization of the ground states  $\Sigma_\alpha^{K^\pm}$  and  $\Sigma_\alpha^{K^0/\bar{K}^0}$ . In the charged kaon condensed phase, we obtain

$$\mathcal{P} = \frac{1}{2} f^2 \mu_{K^\pm,\text{eff}}^2 \left[ 1 - \frac{m_{K^\pm,0}^2}{\mu_{K^\pm,\text{eff}}^2} \right]^2, \quad (164)$$

$$n_I = \frac{1}{2} n_S = \frac{1}{2} f^2 \mu_{K^\pm} \left[ 1 - \frac{m_{K^\pm,0}^4}{\mu_{K^\pm,\text{eff}}^4} \right], \quad (165)$$

where  $\mu_{K^\pm,\text{eff}}^2 = \mu_{K^\pm}^2 - \Delta m_{\text{EM}}^2$ . Finally, in the neutral kaon condensed phase, we find

$$\mathcal{P} = \frac{1}{2} f^2 \mu_{K^0}^2 \left[ 1 - \frac{m_{K^0,0}^2}{\mu_{K^0}^2} \right]^2, \quad (166)$$

$$n_I = -\frac{1}{2} n_S = -\frac{1}{2} f^2 \mu_{K^0} \left[ 1 - \frac{m_{K^0,0}^4}{\mu_{K^0}^4} \right]. \quad (167)$$

In order to find the transition line between two condensed phases, we equate the pressure of them. This gives rise to a line in the phase diagram, which can be solved for one of the chemical potentials as a function of the other chemical potential and the vacuum masses of the condensing modes in adjacent phases. For example, the line between the charged condensed phases satisfies

$$\mu_{K^\pm,\text{eff}} = \pm \frac{1}{2\mu_{I,\text{eff}}} (\mu_{I,\text{eff}}^2 - m_{\pi,0}^2 + \sqrt{(\mu_{I,\text{eff}}^2 - m_{\pi,0}^2)^2 + 4\mu_{I,\text{eff}}^2 m_{K^\pm,0}^2}). \quad (168)$$

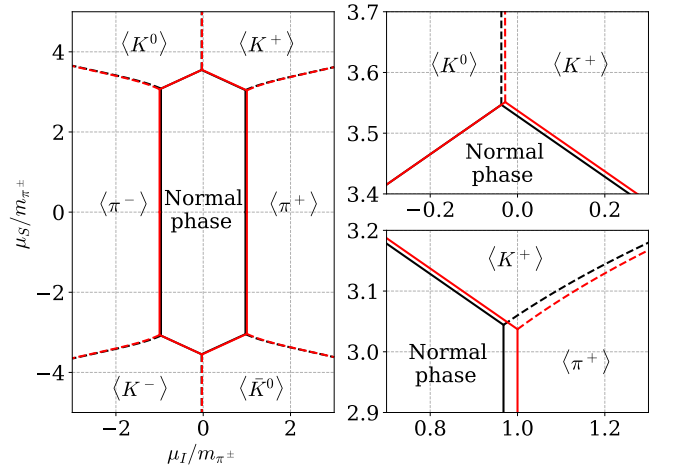


FIG. 5. Left panel: Tree-level phase diagram in the  $\mu_I$ – $\mu_S$  plane. Right panel: zoom in on the triple points. See main text for details.

In Fig. 5, we show the phase diagram in the  $\mu_I$ – $\mu_S$  plane (left panel) and the details near the triple points (right panel). The black lines are without electromagnetic effects and in obtaining the red lines they are included. Solid lines separating the phases indicate that the transition is second order, while dotted lines indicate a first-order transition. In the isospin limit ( $m_u = m_d$ ), this phase diagram was first obtained in Ref. [13]. All the transitions from the vacuum phase are second order, as we have already demonstrated in the transition to the pion-condensed phase. The transitions are in the  $O(2)$  universality class with mean-field exponents. The transitions between the different condensed phases are first order. This can be seen either by a jump in the relevant condensates or by a discontinuity in the relevant rotation

angles. The points where three phases meet (six points) are the triple points.

In the right panel, we notice the small offset between the black and red lines. Since we normalize the chemical potentials to the mass of the charged pion, the lines indicating the onset of charge meson condensation move upon including electromagnetic effects. The electromagnetic interaction increases the effective mass of the charged particles, and as a result, a higher chemical potential is needed for condensation to occur. For example, the vertical line separating the vacuum and the pion-condensed phase is now at

$$\frac{\mu_I^c}{m_{\pi^0,0}} = \frac{m_{\pi^\pm}}{m_{\pi^0,0}} = \sqrt{1 + \frac{\Delta m_{\text{EM}}^2}{m_{\pi^0,0}^2}}. \quad (169)$$

Finally, we notice that the normal phase is independent of the chemical potentials, and so the pressure is constant and the densities vanish in the entire region. This is an example of the so-called Silver Blaze property [27]. More generally, the properties of a specific Bose-condensed phase depend only on a single chemical

potential, namely the relevant one,  $\mu_I$ ,  $\mu_{K^\pm}$ , or  $\mu_{K^0}$ .

## VI. THERMODYNAMICS AT NEXT-TO-LEADING ORDER

In this section, we calculate the pressure at next-to-leading order in the low-energy expansion in the pion-condensed phase. One can obtain similar results for the two kaon-condensed phases. In order to simplify the calculations and to compare our results with lattice simulations, we work in the isospin limit,  $m_u = m_d$ , and ignore electromagnetic effects. From the pressure, we calculate other interesting quantities such as the speed of sound, isospin density, and energy density.

### A. Thermodynamic potential and pressure

There are two contributions to the next-to-leading order thermodynamic potential, namely the static term from  $\mathcal{L}_4$  and the one-loop contribution from  $\mathcal{L}_2$ . The first term reads

$$\Omega_1^{(1)}(\mu_I, \alpha) = -(4L_1 + 4L_2 + 2L_3)\mu_I^4 \sin^4 \alpha - 8L_4 B_0 (2m \cos \alpha + m_s)\mu_I^2 \sin^2 \alpha - 8L_5 B_0 m \mu_I^2 \cos \alpha \sin^2 \alpha - 16L_6 B_0^2 (2m \cos \alpha + m_s)^2 - 8L_8 B_0^2 (2m^2 \cos 2\alpha + m_s^2) - 4H_2 B_0^2 (2m^2 + m_s^2), \quad (170)$$

where  $m = m_u = m_d$ . The one-loop contribution from the quasiparticles is given by

$$\Omega_1^{(2)}(\mu_I, \alpha) = \frac{1}{2} \int_P \log [p_0^2 + E_{\pi^0}^2(p)] + \frac{1}{2} \int_P \log [p_0^2 + E_{\bar{\pi}^\pm}^2(p)] + \frac{1}{2} \int_P \log [p_0^2 + E_{K^\pm}^2(p)] + \frac{1}{2} \int_P \log [p_0^2 + E_{\bar{K}^0/\bar{K}^0}^2(p)] + \frac{1}{2} \int_P \log [p_0^2 + E_\eta^2(p)], \quad (171)$$

where the dispersion relations are given by Eqs. (147)–(150), again with  $\Delta m_{\text{EM}}^2 = 0$ , and we denote the Euclidean four-momentum by  $P^2 = p_0^2 + p^2$ . The shorthand notation for the integral is defined in Eqs. (57)–(58). The first and the last term in Eq. (171) are of the form Eq. (64). Interestingly, the integrals involving the charged and neutral kaons can also be evaluated directly in dimensional regularization. Combining the two contributions from the charged kaons, we find

$$\begin{aligned} \Omega_{1,K^\pm}^{(2)}(\mu_I, \alpha) &= \frac{1}{2} \int_P \log [(P^2 + m_4^2)(P^2 + m_5^2) + p_0^2 m_{45}^2] \\ &= \frac{1}{2} \int_P \log \left\{ \left[ \left( p_0 + \frac{i m_{45}}{2} \right)^2 + p^2 + m_4^2 + \frac{1}{4} m_{45}^2 \right] \left[ \left( p_0 - \frac{i m_{45}}{2} \right)^2 + p^2 + m_4^2 + \frac{1}{4} m_{45}^2 \right] \right\}, \end{aligned} \quad (172)$$

where we in the second line have used  $m_4 = m_5$  and factorized. Shifting the integration variable  $p_0$  in the two terms,  $p_0 \rightarrow p_0 \pm \frac{i}{2} m_{45}$ , we obtain

$$\Omega_{1,K^\pm}^{(2)}(\mu_I, \alpha) = \int_P \log [P^2 + \tilde{m}_4^2], \quad (173)$$

where we have defined  $\tilde{m}_4^2 = m_4^2 + \frac{1}{4} m_{45}^2$ . The contribution from the neutral kaons is given by the same expression with the replacement  $m_6^2 = m_7^2 \rightarrow \tilde{m}_6^2 = m_6^2 + \frac{1}{4} m_{67}^2$ . Finally, consider the contribution from the charged pions. We first rewrite their contribution in the same way as for the charged kaons in Eq. (172),

$$\Omega_{1,\pi^\pm}^{(2)}(\mu_I, \alpha) = \frac{1}{2} \int_P \log [(P^2 + m_1^2)(P^2 + m_2^2) + p_0^2 m_{12}^2]. \quad (174)$$

Since  $m_1 \neq m_2$ , we cannot factorize this expression as we did above. Eq. (174) can thus not be evaluated directly in dimensional regularization. However, using the techniques from Ref. [68], we extract the divergences and express the remainder in terms of a hypergeometric function. Since  $m_1 = 0$  at leading order, the contribution to the pressure is

$$\begin{aligned}\Omega_{1,\pi^\pm}^{(2)}(\mu_I, \alpha_0) &= \frac{1}{2} \int_P \log [P^2(P^2 + m_2^2) + p_0^2 m_{12}^2] \\ &= \frac{1}{2} \int_P \log [P^2 + m_2^2] - \frac{1}{2} \sum_{n=1}^{\infty} \frac{(-1)^n m_{12}^{2n}}{n} \int_P \frac{p_0^{2n}}{P^{2n}(P^2 + m_2^2)^n},\end{aligned}\quad (175)$$

where we in the second line have expanded the logarithm. Averaging Eq. (175) over angles, we find

$$\Omega_{1,\pi^\pm}^{(2)}(\mu_I, \alpha_0) = -\frac{1}{2} I_0'(m_2^2) - \frac{\Gamma(2-\epsilon)}{2\Gamma(\frac{1}{2})} \sum_{n=1}^{\infty} \frac{\Gamma(n+\frac{1}{2})}{\Gamma(n+2-\epsilon)} \frac{(-1)^n m_{12}^{2n}}{n} I_n(m_2^2), \quad (176)$$

where the integrals  $I_0'(m^2)$  and  $I_n(m^2)$  are defined in Eqs. (59)–(60). We single out the divergent terms in the series ( $n = 1, 2$ ) and set  $d = 3$  in the remainder ( $n \geq 3$ ). Redefining the dummy index  $n$  and introducing the Pochhammer symbol  $(a)_b = \Gamma[a+b]/\Gamma[a]$ , we can write

$$\Omega_{1,\pi^\pm}^{(2)}(\mu_I, \alpha_0) = -\frac{1}{2} I_0'(m_2^2) + \frac{m_{12}^2}{2(d+1)} I_1(m_2^2) - \frac{3m_{12}^4}{4(d+1)(d+3)} I_2(m_2^2) + \frac{5m_{12}^6}{768(4\pi)^2 m_2^2} \sum_{n=0}^{\infty} \frac{(1)_n (1)_n (\frac{7}{2})_n}{(4)_n (5)_n} \frac{(-\frac{m_{12}^2}{m_2^2})^n}{n!}. \quad (177)$$

The expression Eq. (177) is identified as the series expansion of a hypergeometric function  ${}_3F_2$  [69], and we obtain

$$\Omega_{1,\pi^\pm}^{(2)}(\mu_I, \alpha_0) = -\frac{1}{2} I_0'(m_2^2) + \frac{m_{12}^2}{2(d+1)} I_1(m_2^2) - \frac{3m_{12}^4}{4(d+1)(d+3)} I_2(m_2^2) + \frac{5m_{12}^6}{768(4\pi)^2 m_2^2} {}_3F_2 \left[ \begin{matrix} 1, & 1, & \frac{7}{2} \\ & 4, & 5 \end{matrix} \middle| -\frac{m_{12}^2}{m_2^2} \right]. \quad (178)$$

The hypergeometric function  ${}_3F_2$  has a closed-form expression

$${}_3F_2 \left[ \begin{matrix} 1, & 1, & \frac{7}{2} \\ & 4, & 5 \end{matrix} \middle| z \right] = \frac{16}{5} \left[ \frac{(3z^2 - 10z - 8)(1 - \sqrt{1-z})}{z^4} + \frac{z^2 + 4}{z^3} - 3 \frac{z^2 - 4z + 8}{z^3} \log \frac{1 + \sqrt{1-z}}{2} \right]. \quad (179)$$

Adding the contributions, renormalizing the bare couplings according to Eqs. (29)–(30), and evaluating the expressions for  $\cos \alpha_0 = \frac{m_{\pi,0}^2}{\mu_I^2}$  we obtain the next-to-leading order pressure. In the final result, we subtract the vacuum pressure. This yields

$$\begin{aligned}\mathcal{P}_{0+1} &= \frac{1}{2} f^2 \mu_I^2 \left[ 1 - \frac{m_\pi^2}{\mu_I^2} \right] - \frac{1}{2} f^2 \frac{m_{\pi,0}^4}{m_\pi^2} \left[ 1 - \frac{m_\pi^2}{\mu_I^2} \right] \\ &+ \left[ 4L_1^r + 4L_2^r + 2L_3^r + \frac{1}{4(4\pi)^2} \left( \log \frac{\Lambda^2}{m_2^2} + \log \frac{\Lambda^2}{m_3^2} + \frac{1}{4} \log \frac{\Lambda^2}{\tilde{m}_4^2} + \frac{9}{8} \right) \right] \mu_I^4 \\ &- \left[ 32L_6^r + \frac{1}{(4\pi)^2} \left( \log \frac{\Lambda^2}{m_{K,0}^2} + \frac{2}{9} \log \frac{\Lambda^2}{m_{\eta,0}^2} + \frac{11}{18} \right) \right] m_{\pi,0}^2 \tilde{m}_{K,0}^2 \\ &- \left[ 8L_1^r + 8L_2^r + 4L_3^r - 8L_4^r - 4L_5^r + 16L_6^r + 8L_8^r \right. \\ &+ \left. \frac{1}{4(4\pi)^2} \left( 3 \log \frac{\Lambda^2}{m_{\pi,0}^2} + \log \frac{\Lambda^2}{m_{K,0}^2} - \frac{1}{2} \log \frac{\Lambda^2}{\tilde{m}_4^2} + \frac{1}{9} \log \frac{\Lambda^2}{m_{\eta,0}^2} + \frac{65}{36} \right) \right] m_{\pi,0}^4 \\ &+ \frac{1}{(4\pi)^2} \left[ \log \frac{m_{K,0}^2}{\tilde{m}_4^2} + \frac{4}{9} \log \frac{m_{\eta,0}^2}{m_8^2} \right] \tilde{m}_{K,0}^4 \\ &- \left[ 8L_4^r - 32L_6^r - \frac{1}{2(4\pi)^2} \left( \log \frac{\Lambda^2}{\tilde{m}_4^2} + \frac{4}{9} \log \frac{\Lambda^2}{m_8^2} + \frac{13}{18} \right) \right] \frac{m_{\pi,0}^4 \tilde{m}_{K,0}^2}{\mu_I^2}\end{aligned}$$



$$\begin{aligned}
& + \left[ 4L_1^r + 4L_2^r + 2L_3^r - 8L_4^r - 4L_5^r + 16L_6^r + 8L_8^r \right. \\
& + \frac{1}{144(4\pi)^2} \left( 36 \log \frac{\Lambda^2}{m_2^2} + 9 \log \frac{\Lambda^2}{\tilde{m}_4^2} + 4 \log \frac{\Lambda^2}{m_8^2} - \frac{47}{2} \right) \left. \frac{m_{\pi,0}^8}{\mu_I^4} \right] \\
& + \left[ 8L_4^r + \frac{1}{2(4\pi)^2} \left( \log \frac{\Lambda^2}{\tilde{m}_4^2} + \frac{1}{2} \right) \right] \tilde{m}_{K,0}^2 \mu_I^2 \\
& - \frac{5m_{\pi,0}^{12}}{12(4\pi)^2(\mu_I^4 - m_{\pi,0}^4)\mu_I^4} {}_3F_2 \left[ \begin{matrix} 1, & 1, & \frac{7}{2} \\ 4, & 5 \end{matrix} \middle| -\frac{4m_{\pi,0}^4}{\mu_I^4 - m_{\pi,0}^4} \right], \tag{180}
\end{aligned}$$

where the masses in Eqs. (136)–(138), (140), and (144) are evaluated at  $\cos \alpha_0 = \frac{m_{\pi,0}^2}{\mu_I^2}$ ,

$$m_2^2 = \mu_I^2 \left[ 1 - \frac{m_{\pi,0}^4}{\mu_I^4} \right], \tag{181}$$

$$m_3^2 = \mu_I^2, \tag{182}$$

$$\tilde{m}_4^2 = m_4^2 + \frac{1}{4}m_{45}^2 = \tilde{m}_{K,0}^2 + \frac{1}{4}\mu_I^2 \left[ 1 + \frac{m_{\pi,0}^4}{\mu_I^4} \right], \tag{183}$$

$$m_8^2 = m_{\eta,0}^2 - \frac{1}{3}m_{\pi,0}^2 \left[ 1 - \frac{m_{\pi,0}^2}{\mu_I^2} \right] = \frac{1}{3} \left[ 4\tilde{m}_{K,0}^2 + \frac{m_{\pi,0}^4}{\mu_I^2} \right], \tag{184}$$

with  $\tilde{m}_{K,0}^2 = B_0 m_s$ . In Eq. (180), we have subtracted a constant such that the pressure vanishes at  $\mu_I = m_{\pi}$ . No-

tice that the explicit  $\Lambda$ -dependence in Eq. (180) cancels against the  $\Lambda$ -dependence of the renormalized couplings  $L_i^r$  as given by Eq. 37. This remark about the independence of the renormalization scale applies to all physical quantities.

## B. Large $m_s$ -mass limit

The three-flavor pressure is given in Eq. (180). In the large- $m_s$  limit, one expects that the kaons and the eta decouple, and to recover the two-flavor result for the pressure (and all other thermodynamic quantities). The effect of the  $s$ -quark in this limit is simply to renormalize the couplings, a result one would obtain by integrating it out at the level of the Lagrangian to obtain a low-energy effective theory for the light mesons. Expanding the three-flavor pressure in inverse powers of  $B_0 m_s$  and throwing away terms that only depend on  $m_s$ , we obtain

$$\begin{aligned}
\mathcal{P}_{0+1} & = \frac{1}{2}\tilde{f}^2 \mu_I^2 \left[ 1 - \frac{m_{\pi}^2}{\mu_I^2} \right] - \frac{1}{2}\tilde{f}^2 \frac{\tilde{m}_{\pi,0}^4}{m_{\pi}^2} \left[ 1 - \frac{m_{\pi}^2}{\mu_I^2} \right] - m_{\pi,0}^4 \left[ 2l_1^r + 2l_2^r + l_3^r + \frac{3}{4(4\pi)^2} \left( \log \frac{\Lambda^2}{m_{\pi,0}^2} + \frac{1}{2} \right) \right] \\
& + \frac{m_{\pi,0}^8}{\mu_I^4} \left[ l_1^r + l_2^r + l_3^r + \frac{1}{4(4\pi)^2} \left( \log \frac{\Lambda^2 \mu_I^2}{\mu_I^4 - m_{\pi,0}^4} - \frac{5}{6} \right) \right] + \mu_I^4 \left[ l_1^r + l_2^r + \frac{1}{4(4\pi)^2} \left( \log \frac{\Lambda^4}{\mu_I^4 - m_{\pi,0}^4} + 1 \right) \right] \\
& - \frac{5m_{\pi,0}^{12}}{12(4\pi)^2(\mu_I^4 - m_{\pi,0}^4)\mu_I^4} {}_3F_2 \left[ \begin{matrix} 1, & 1, & \frac{7}{2} \\ 4, & 5 \end{matrix} \middle| -\frac{4m_{\pi,0}^4}{\mu_I^4 - m_{\pi,0}^4} \right]. \tag{185}
\end{aligned}$$

where we have defined the renormalized parameters

$$\tilde{B}_0 m = B_0 m \left[ 1 - \left( 16L_4^r - 32L_6^r - \frac{2}{9(4\pi)^2} \log \frac{\Lambda^2}{\tilde{m}_{\eta,0}^2} \right) \frac{\tilde{m}_{K,0}^2}{f^2} \right], \tag{186}$$

$$\tilde{f}^2 = f^2 \left[ 1 + \left( 16L_4^r + \frac{1}{(4\pi)^2} \log \frac{\Lambda^2}{\tilde{m}_{K,0}^2} \right) \frac{\tilde{m}_{K,0}^2}{f^2} \right], \quad (187)$$

$$l_1^r + l_2^r = 4L_1^r + 4L_2^r + 2L_3^r + \frac{1}{16(4\pi)^2} \left[ \log \frac{\Lambda^2}{\tilde{m}_{K,0}^2} - 1 \right], \quad (188)$$

$$l_3^r = -8L_4^r - 4L_5^r + 16L_6^r + 8L_8^r + \frac{1}{36(4\pi)^2} \left[ \log \frac{\Lambda^2}{\tilde{m}_{\eta,0}^2} - 1 \right], \quad (189)$$

with  $\tilde{m}_{\pi,0}^2 = 2\tilde{B}_0 m$  and  $\tilde{m}_{\eta,0}^2 = \frac{4}{3}B_0 m_s$ . Comparing Eqs. (186) and (187) with Eqs. (190) and (192) below, we see that  $\tilde{B}_0 m$  and  $\tilde{f}$  contain exactly the one-loop corrections to the pion mass and the pion decay constant from the heavy mesons. Eqs. (188) and (189) are in agreement with the result obtained by Gasser and Leutwyler in Ref. [10] when comparing two and three-flavor  $\chi$ PT in the large  $m_s$ -mass limit. Eq. 185 is in agreement with the recent two-flavor result of Ref. [33] after the identification of  $\tilde{f}$  and  $\tilde{B}_0 m$  as parameters including renormalization effects from  $s$ -quark loops.

### C. Numerical results

We have expressed our result Eq. (180) for the pressure in terms of the bare masses  $m_{\pi,0}$  and  $m_{K,0}$ , the bare decay constant  $f$ , the renormalized couplings  $L_i^r(\Lambda)$ , and the isospin chemical potential  $\mu_I$ . In order to evaluate numerically thermodynamic quantities such as the pressure and the energy density consistently, we need to re-

late the physical masses (pole masses) to the bare ones. At leading order, this was straightforward as shown in section V A. At next-to-leading order, this requires that we determine these relations also at next-to-leading order. We therefore need the pole masses calculated to one-loop order. Similarly, the relation between the measured pion decay constant  $f_\pi$  and its bare counterpart  $f$  receives radiative corrections. The relations are [10]

$$m_\pi^2 = m_{\pi,0}^2 \left[ 1 - \left( 8L_4^r + 8L_5^r - 16L_6^r - 16L_8^r + \frac{1}{2(4\pi)^2} \log \frac{\Lambda^2}{m_{\pi,0}^2} \right) \frac{m_{\pi,0}^2}{f^2} - (L_4^r - 2L_6^r) \frac{16m_{K,0}^2}{f^2} + \frac{m_{\eta,0}^2}{6(4\pi)^2 f^2} \log \frac{\Lambda^2}{m_{\eta,0}^2} \right], \quad (190)$$

$$m_K^2 = m_{K,0}^2 \left[ 1 - (L_4^r - 2L_6^r) \frac{8m_{\pi,0}^2}{f^2} - (2L_4^r + L_5^r - 4L_6^r - 2L_8^r) \frac{8m_{K,0}^2}{f^2} - \frac{m_{\eta,0}^2}{3(4\pi)^2 f^2} \log \frac{\Lambda^2}{m_{\eta,0}^2} \right], \quad (191)$$

$$f_\pi^2 = f^2 \left[ 1 + \left( 8L_4^r + 8L_5^r + \frac{2}{(4\pi)^2} \log \frac{\Lambda^2}{m_{\pi,0}^2} \right) \frac{m_{\pi,0}^2}{f^2} + \left( 16L_4^r + \frac{1}{(4\pi)^2} \log \frac{\Lambda^2}{m_{K,0}^2} \right) \frac{m_{K,0}^2}{f^2} \right]. \quad (192)$$

Since we are working in the isospin limit and with  $e = 0$  limit, we only need two physical masses, in contrast to the four used in V A. In addition, we need the physical value of  $f_\pi$  and the experimental values for the renormalized couplings at a certain scale. For three flavors, the convention is that the running couplings are measured at the scale  $\Lambda = m_\rho = 770$  MeV. The couplings needed are listed in Table I, taken from Ref. [70].

In Table II, we show the LO and NLO values for the bare parameters. At LO the bare parameters are equal to the experimental values as explained. At NLO, they are obtained by solving Eqs. (190)–(192) numerically using the physical values for  $m_\pi$ ,  $m_K$ ,  $f_\pi$ , and  $L_i^r$  as input.

Since we will be comparing our results with recent lattice simulations [25], we use their values for the masses and the pion decay constant and not the values tabulated by the Particle Data Group [66]. The values are  $m_\pi = 135.0$  MeV and  $m_K = 495.0$  MeV. The simulations are carried out with two different lattices,  $24^3 \times 32$  and  $32^3 \times 48$  and with  $f_\pi = \frac{130}{\sqrt{2}}$  and  $f_\pi = \frac{136}{\sqrt{2}}$ , respectively. We choose  $f_\pi = \frac{133}{\sqrt{2}}$  as reasonable value. At NLO, the pion-decay constant and the mass of kaon receive significant radiative corrections, while the pion mass is hardly affected.

In the upper left panel of Fig. 6, we show the LO (black dashed line) and NLO (red solid line) results for the pres-

sure  $\mathcal{P}$  normalized to  $\mathcal{P}_0 = f_\pi^2 m_\pi^2$  as a function of  $\mu_I/m_\pi$ . In the remaining panels, we show the LO and NLO results

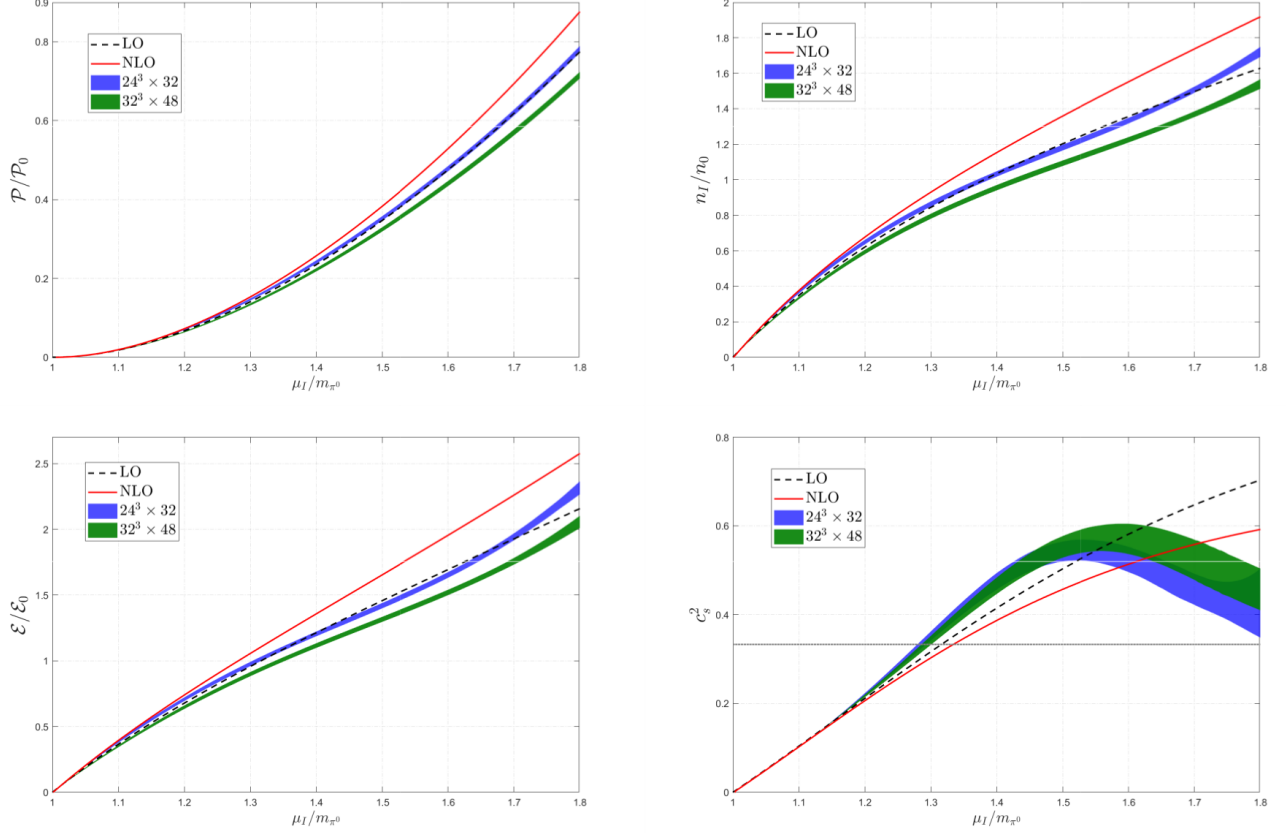


FIG. 6. LO and NLO results for the normalized pressure, isospin density, energy density, and speed of sound squared, all functions of the normalized isospin chemical potential  $\mu_I/m_\pi$ , where  $m_\pi$  is the physical pion mass at the same order as the approximation. See main text for details.

Constant	Value [ $\times 10^{-3}$ ]	Source
$L_1^r(\Lambda)$	$1.0 \pm 0.1$	[70]
$L_2^r(\Lambda)$	$1.6 \pm 0.2$	[70]
$L_3^r(\Lambda)$	$-3.8 \pm 0.3$	[70]
$L_4^r(\Lambda)$	$0.0 \pm 0.3$	[70]
$L_5^r(\Lambda)$	$1.2 \pm 0.1$	[70]
$L_6^r(\Lambda)$	$0.0 \pm 0.4$	[70]
$L_8^r(\Lambda)$	$0.5 \pm 0.2$	[70]

TABLE I. The renormalized coupling constants  $L_i^r(\Lambda)$  of the next-to-leading order Lagrangian of three-flavor chiral perturbation theory, measured at the scale of the  $\rho$  meson,  $\Lambda = m_\rho$ .

for the normalized isospin density (upper right panel), normalized energy density (lower left panel), and speed of sound squared  $c_s^2$  (lower right panel) as functions of  $\mu_I/m_\pi$ , with the same color coding. The energy density is normalized to  $\mathcal{E}_0 = f_\pi^2 m_\pi^2$  and the isospin density to  $n_0 = f_\pi^2 m_\pi$ . The horizontal grey line in the lower right panel is the speed of sound in the conformal limit,  $c_s = \frac{1}{\sqrt{3}}$ . Note that since we have normalized the isospin chemical potential to the physical pion mass determined

Bare parameter	LO [MeV]	NLO [MeV]	1 - LO/NLO
$m_{\pi,0}$	135.0	135.5	0.004
$m_{K,0}$	495.0	529.4	0.0649
$f$	$133/\sqrt{2} \approx 94.0$	80.8	-0.164

TABLE II. Leading order and next-to-leading order values for the bare masses and decay constant. The values are for  $\Delta m^2 = 0$  and  $\Delta m_{\text{EM}}^2 = 0$ . The physical values, equal to the LO values, are those used in lattice simulations [25].

at the same order as the approximation for the quantity in question, the transition takes place exactly at  $\mu_I/m_\pi = 1$ . The correction going from LO to NLO is increasing as we increase  $\mu_I$  and is rather modest for values up to  $\mu_I \approx 1.3m_\pi$ . For the sake of numerical evaluation, all NLO contributions in Eq. (180) have been evaluated at the physical masses. That is, from line two and below, we make the substitution  $m_{\pi,0} \rightarrow m_\pi$ , and so on. This is consistent to the order in  $\chi$ PT we are working.

We also compare our results with two sets of lattice data from Ref. [25]. The simulations are done on a  $24^3 \times 32$  (blue) and a  $32^3 \times 48$  lattice (green), respectively, where the bands indicate the errors. We remark

in passing that in Ref. [25], the pressure and energy density are normalized to  $m_\pi^4$  instead of  $f_\pi^2 m_\pi^2$  and the plots therefore look somewhat different. The predictions from  $\chi$ PT are in good agreement for values of  $\mu_I$  up to approximately  $1.3m_\pi$ , somewhat dependent on the quantity in question. Generally, in the region where the NLO results start to deviate from the LO results, the latter is in better agreement with Monte Carlo simulations. This is in contrast to the predictions for the quark and pion condensates [32], here the NLO results are in significantly better agreement with lattice results.

The plot of the speed of sound squared is perhaps particularly interesting. The prediction from  $\chi$ PT is in good agreement with lattice for  $\mu_I$  up to values of perhaps  $1.3m_\pi$ , whereafter  $\chi$ PT fails badly: The speed of sound increases, as we increase the chemical potential, while the lattice results show a peak around  $\mu_I = 1.55m_\pi$ , after which it decreases.  $\chi$ PT is described by an EoS that in the ultrarelativistic limit is  $\epsilon = p$  and therefore the speed of sound approaches the speed of light as  $\mu_I \rightarrow \infty$ . In contrast to this, in lattice QCD, the relevant degrees at high isospin density are fermions. The EoS of an ideal Fermi gas is  $\epsilon = 3p$  and the speed of sound is  $c_s = \frac{1}{\sqrt{3}}$ , which is the conformal limit. Due to asymptotic freedom, it is expected that QCD approaches this limit as the density increases and the strong interaction gets weaker. Perturbative QCD can be applied for very large values of  $\mu_I$ . In a recent paper [71], the authors use the Cornwall-Jackiw-Tomboulis (CJT) formalism [72] to study the behavior of  $c_s$  for large  $\mu_I$ . The speed of sound does approach the conformal limit, but the way depends on whether one includes the BCS gap or not: Including the gap  $c_s$  approaches  $\frac{1}{\sqrt{3}}$  from above, otherwise  $c_s$  approaches the conformal limit from below.

## VII. CHIRAL LIMIT OF TWO-FLAVOR $\chi$ PT

In two-flavor  $\chi$ PT at finite  $\mu_I$ , there are three mass scales, namely the pion mass, the pion decay constant, and the isospin chemical potential. In the chiral limit, we have only two mass scales  $f$  and  $\mu_I$ , and a single dimensionless ratio, namely  $\mu_I/f$ . All thermodynamic quantities can therefore be expanded in this ratio, and higher-order calculations are in fact tractable. The main reason is that the propagator is diagonal and has a simple form due to the fact that  $\alpha = \frac{1}{2}\pi$ . It then follows that the LO pressure is  $\mathcal{P}_0 = \frac{1}{2}f^2\mu_I^2$  and the pressure can be written as a series

$$\mathcal{P}_{0+1+2+\dots} = \frac{1}{2}f^2\mu_I^2 + a_1\mu_I^4 + a_2\frac{\mu_I^6}{f^2} + \dots, \quad (193)$$

where  $a_i$  ( $i = 1, 2, \dots$ ) are coefficients. The pressure through  $\mathcal{O}(p^4)$  in the chiral limit can be found by sending the bare pion mass  $m_{\pi,0}$  to zero in Eq. (185) and ignoring the loop correction from the  $s$ -quark to  $f$  in Eq. (187). Noting that the contribution from the hypergeometric function vanishes in this limit, we obtain the coefficient  $a_1$

$$a_1 = l_1^r(\Lambda) + l_2^r(\Lambda) + \frac{1}{2(4\pi)^2} \left[ \log \frac{\Lambda^2}{\mu_I^2} + \frac{1}{2} \right]. \quad (194)$$

The scale dependence of the running couplings  $l_1^r(\Lambda)$  and  $l_2^r(\Lambda)$  in Eq. (194) cancels against the explicit scale dependence of  $\log \frac{\Lambda^2}{\mu_I^2}$  in such a way that  $a_1$  is independent of  $\Lambda$ . This remark also applies to  $a_2, a_3, \dots$ , and ensures the scale independence of the pressure order by order in the low-energy expansion.

The cubic and quartic interactions from the LO Lagrangian are

$$\mathcal{L}_2^{(3)} = \frac{\mu_I}{f} \partial_0 \phi_1 [\phi_2^2 + \phi_3^2], \quad (195)$$

$$\mathcal{L}_2^{(4)} = \frac{1}{6f^2} [\phi_a \phi_b (\partial_\mu \phi_a) (\partial^\mu \phi_b) - \phi_a \phi_a (\partial_\mu \phi_b) (\partial^\mu \phi_b)] + \frac{\mu_I^2}{6f^2} \phi_a \phi_a [\phi_2^2 + \phi_3^2]. \quad (196)$$

The NLO Lagrangian Eq. (39) is expanded to second order in  $\phi_a$ , which gives

$$\mathcal{L}_4^{(2)} = -2(l_1 + l_2) \frac{\mu_I^4}{f^2} (\phi_2^2 + \phi_3^2) + 2(2l_1 + l_2) \frac{\mu_I^2}{f^2} (\partial_0 \phi_1)^2 + 2l_1 \frac{\mu_I^2}{f^2} (\partial_\mu \phi_a) (\partial^\mu \phi_a) + 2l_2 \frac{\mu_I^2}{f^2} [(\partial_\mu \phi_1) (\partial^\mu \phi_1) + (\partial_0 \phi_a)^2] \quad (197)$$

The order- $p^6$  contributions to the pressure from one-loop graphs with counterterm insertions and two-loop graphs are

$$\begin{aligned} \mathcal{P}_2^{\text{loops}} &= \frac{\mu_I^2}{6f^2} [3I_1^2(m_2^2) + 3I_1^2(m_3^2) + 2I_1(m_2^2)I_1(m_3^2)] - \frac{1}{6f^2} [m_2^2 + m_3^2] I_1(m_2^2)I_1(m_3^2) \\ &\quad - \frac{\mu_I^2}{f^2} [J(m_2^2) + J(m_3^2)] - 2(l_1 + l_2) \frac{\mu_I^4}{f^2} [I_1(m_2^2) + I_1(m_3^2)] \\ &\quad + 2l_1 \frac{\mu_I^2}{f^2} [m_2^2 I_1(m_2^2) + m_3^2 I_1(m_3^2)] + 2l_2 \frac{\mu_I^2}{f^2} \left[ \frac{m_2^2}{d+1} I_1(m_2^2) + \frac{m_3^2}{d+1} I_1(m_3^2) \right], \end{aligned} \quad (198)$$

where the integral  $J(m^2)$  is defined in Eq. (67). Coun-

terterm diagrams with a massless propagator or double-

bubble diagrams with a massless propagator vanish in dimensional regularization since there is no mass scale in the corresponding integrals. Contributions from these diagrams are not included in Eq. (198) above. Using the fact that  $m_2 = m_3 = \mu_I$  and the expression for  $J(m^2)$  in Eq. (68), Eq. (198) reduces to

$$\mathcal{P}_2^{\text{loops}} = \frac{d-1}{d+1} \frac{\mu_I^2}{f^2} I_1^2(\mu_I^2) - l_2 \frac{4d}{d+1} \frac{\mu_I^4}{f^2} I_1(\mu_I^2). \quad (199)$$

Note that the dependence on  $l_1$  drops out. The contribution to the pressure from the static part of  $\mathcal{L}_6$  is

$$\mathcal{P}_2^{\text{static}} = 2(C_{24} + C_{25} + C_{26})\mu_I^6. \quad (200)$$

Adding Eqs. (199) and (200), renormalizing  $\mathcal{C} = C_{24} + C_{25} + C_{26}$  according to Eq. (46), we obtain the NNLO contribution to the pressure. The coefficient  $a_2$  reads

$$a_2 = 2C_r - \frac{1}{(4\pi)^2} \left[ \frac{1}{2} - 3 \log \frac{\Lambda^2}{\mu_I^2} \right] l_2^r + \frac{1}{(4\pi)^4} \left[ -\frac{1}{24} - \frac{1}{3} \log \frac{\Lambda^2}{\mu_I^2} + \frac{1}{2} \log^2 \frac{\Lambda^2}{\mu_I^2} \right] \quad (201)$$

It can be verified that  $a_2$  is independent of the scale  $\Lambda$  using the running of  $l_2^r(\Lambda)$  and  $C^r(\Lambda)$ . Comparing the coefficients  $a_1$  and  $a_2$ , we note that the effective expansion parameter is  $\mu_I^2/(4\pi)^2 f^2$ . This suggests that the chiral limit should be a good approximation for  $m_\pi \ll \mu_I \ll 4\pi f$ .

### VIII. LOW-ENERGY EFFECTIVE THEORY AND PHONON DAMPING RATE

In section V, we calculated the dispersion relations for the charged and neutral mesons in the pion-condensed phase at leading order in the low-energy expansion. The Goldstone mode has a linear dispersion relation for small momentum  $p$ , which follows directly from a Taylor expansion of the dispersion relation Eq. (148) around  $p = 0$ ,

$$E_{\pi^-}(p) = \sqrt{\frac{\mu_I^4 - m_{\pi,0}^4}{\mu_I^4 + 3m_{\pi,0}^4}} p + \mathcal{O}(p^2), \quad (202)$$

where  $m_{\pi,0}$  is the mass of the charged pion mass at tree level. More generally, one can ask about the low-energy dynamics and the low-energy effective theory that describes the Goldstone boson or phonon alone. Let us for simplicity discuss the two-flavor case. Since the massive excitations have masses of  $\mu_I$  and  $\mu_I \sqrt{\frac{\mu_I^4 + 3m_{\pi,0}^4}{\mu_I^4}}$  in the broken phase, the low-energy effective theory will be valid for  $p \ll \mu_I$ . In the case of a single chemical potential  $\mu$  and a Goldstone boson  $\phi$  associated with the breaking of a  $U(1)$  symmetry, Son showed how to construct such a theory more than two decades ago [73]. The prescription is remarkably simple: The effective theory for the GB  $\phi$  is given in terms of the thermodynamic pressure  $\mathcal{P}$  as a

function of the chemical potential  $\mu$  and possibly other quantities such as meson masses simply by making the substitution  $\mu \rightarrow \sqrt{\nabla_\mu \phi \nabla^\mu \phi}$ , i.e.

$$\mathcal{L} = \mathcal{P}(\mu \rightarrow \sqrt{\nabla_\mu \phi \nabla^\mu \phi}), \quad (203)$$

where the covariant derivative is  $\nabla_\mu \phi = \partial_\mu \phi - \delta_{\mu 0} \mu$ . The only assumption that was made is that the dispersion relation for the phonon is linear. Eq. (202) is only linear for small momenta and once there are sizable corrections, the effective theory breaks down.<sup>6</sup> Making the substitution Eq. (203) in the LO pressure Eq. (162) with  $\Delta m_{\text{EM}}^2 = 0$ , expanding the Lagrangian in powers of derivatives, and rescaling the field, we obtain

$$\mathcal{L} = \frac{1}{2}(\partial_0 \phi)^2 - \frac{1}{2}c_s^2(\nabla \phi)^2 + c_1(\partial_0 \phi)^3 + c_1 \partial_0 \phi (\nabla \phi)^2 + \dots, \quad (204)$$

where we have omitted a linear term and the ellipses indicate higher-order operators. The phonon speed  $c_s$  and the coupling  $c_1$  are

$$c_s = \sqrt{\frac{\mu_I^4 - m_{\pi,0}^4}{\mu_I^4 + 3m_{\pi,0}^4}}, c_1 = \frac{2m_{\pi,0}^4 \mu_I}{f} \frac{1}{(\mu_I^4 + 3m_{\pi,0}^4)^{\frac{3}{2}}}. \quad (205)$$

We next consider loop corrections to the dispersion relation. In order to calculate the full self-energy at one loop, we need the quartic terms in the expansion Eq. (204), however, the corresponding diagrams contribute only to its real part. The corresponding correction is simply a correction to the phonon speed which can also be calculated directly from the equation of state. In order to calculate the imaginary part and hence the damping rate, it is sufficient to consider the cubic terms. Our calculations closely follow those of Refs. [74–76], in which the leading-order phonon speed and the damping rate in the color-flavor-locked phase of QCD were calculated. The expression for the relevant self-energy diagram is given by the following integral in Euclidean space

$$\Pi(P) = c_1^2 \int_Q \frac{F(P, Q)}{(q_0^2 + c_s^2 q^2)[(p_0 - q_0)^2 + c_s^2(\mathbf{p} - \mathbf{q})^2]} \quad (206)$$

where the function  $F(P, Q)$  is defined as

$$F(P, Q) = 2 \{ 3(p_0 - q_0)p_0 q_0 - (p_0 - q_0)\mathbf{p} \cdot \mathbf{q} - p_0(\mathbf{p} \cdot \mathbf{q} - q^2) - q_0(p^2 - \mathbf{p} \cdot \mathbf{q}) \}^2 \quad (207)$$

The integral is next rewritten using Feynman parameters, changing the variables  $R = Q - Px$  and scaling  $r_0, r_0 \rightarrow r_0/c_s$ . The leading contribution is obtained by setting

<sup>6</sup> For a color superconductor, the momenta must be much smaller than the superconducting gap  $\Delta$ . For a dilute Bose see section IX A.

$R = 0$  in the numerator. The function  $F(P, R)$  then reduces to  $G(P) = F(P, 0)$ , where

$$G(P) = 18x^2(1-x)^2 p_0^2(p_0^2 + p^2)^2. \quad (208)$$

This yields

$$\Pi(P) = \frac{c_1^2}{c_s^3} \int_0^1 dx \int_R \frac{G(P)}{\left[ R^2 + \frac{p_0^2 + c_s^2 p^2}{c_s^2} x(1-x) \right]^2} \quad (209)$$

We next use Eq. (66) for the integral of momenta  $R$ . Integrating the resulting expression with respect to  $x$  and going back to Minkowski space,  $ip_0 \rightarrow \omega + i\epsilon$  yields

$$\begin{aligned} \Pi(\omega, p) = & -\frac{3c_1^2}{5(4\pi)^2 c_s^3} \omega^2 (\omega^2 - p^2)^2 \\ & \times \left[ \frac{1}{\epsilon} - \log \frac{\omega^2 - c_s^2 p^2}{c_s^2 \Lambda^2} + \frac{47}{30} + i\pi \right]. \end{aligned} \quad (210)$$

The damping rate  $\gamma$  is defined as

$$\gamma = - \left. \frac{\text{Im}\Pi(\omega, p)}{\omega} \right|_{\omega^2 = c_s^2 p^2}. \quad (211)$$

In the nonrelativistic limit,  $c_s^2 \ll 1$ , and we can approximate  $(\omega^2 - p^2)^2$  by  $p^4$ , which yields

$$\gamma = \frac{3c_1^2}{160\pi c_s^2} p^5. \quad (212)$$

In the nonrelativistic limit,  $c_s^2 \rightarrow \frac{n_I}{4m_{\pi,0} f^2}$  and  $c_1 \rightarrow \frac{1}{4fm_{\pi,0}}$ , which follows from Eq. (205) and the results on the dilute Bose gas in the next section. This yields

$$\gamma = \frac{3p^5}{640\pi m_{\pi,0} n_I}, \quad (213)$$

which is the classic result by Beliaev [77] for a dilute Bose gas. In the next section, we discuss the dilute Bose gas and the nonrelativistic limit of  $\chi$ PT further.

## IX. DILUTE BOSE GAS AND THE NONRELATIVISTIC LIMIT OF $\chi$ PT

In this section, we first briefly discuss the classic textbook example of Bose condensation, namely that of a nonrelativistic dilute Bose gas [78]. The leading correction to the energy density is derived using effective field theory methods. We then show that a pion condensate behaves nonrelativistically close to the phase transition [79]. Finally, we recover the two-flavor results from Ref. [33] by taking the limit  $m_s \rightarrow \infty$ .

### A. Dilute Bose gas

The dilute Bose gas has been studied extensively for several decades beginning with the paper by Bogoliubov [80] in 1947. The starting point is a nonrelativistic

low-energy effective field theory that describes the particles at momenta much lower than the inverse of the range of their interactions [81]. The Lagrangian that describes the system at finite number density is

$$\begin{aligned} \mathcal{L} = & \psi^\dagger (i\partial_0 + \mu_{\text{NR}}) \psi - \frac{1}{2m} \nabla \psi^\dagger \cdot \nabla \psi - \frac{1}{4} g (\psi^\dagger \psi)^2 \\ & - \frac{1}{4} h [\nabla(\psi^\dagger \psi)]^2 - \frac{1}{36} g_3 (\psi^\dagger \psi)^3 + \dots, \end{aligned} \quad (214)$$

where the quantum field  $\psi^\dagger$  creates a particle,  $\psi$  destroys a particle,  $\mu_{\text{NR}}$  is the nonrelativistic chemical potential,  $g$ , and  $g_3$  are coupling constants. The ellipses indicate terms that are of higher order in the number fields  $\psi$ ,  $\psi^\dagger$  and/or their derivatives. The term  $(\psi^\dagger \psi)^2$  represents  $2 \rightarrow 2$  scattering and the coupling  $g$  is related to the  $s$ -wave scattering length  $a$  as  $g = \frac{8\pi a}{m}$ . The term  $\frac{1}{4} h [\nabla(\psi^\dagger \psi)]^2$  includes the effective range  $r_s$  of the two-body potential, where  $h = 2\pi a^2 r_s$ . The term  $(\psi^\dagger \psi)^3$  represents  $3 \rightarrow 3$  scattering.

At zero temperature, the expansion parameter of the dilute Bose gas is the so-called (dimensionless) gas parameter  $\sqrt{na^3}$ , where  $n$  is the number density. Bogoliubov [80] obtained the mean-field results for the pressure, number density, and energy density. For example, the energy density is  $\mathcal{E}(n) = \frac{2\pi a n^2}{m}$ . The leading corrections to Bogoliubov's result for the energy density were calculated by Lee, Huang, and Yang [82, 83] for a hard-sphere potential. Later, part of the next-to-leading order correction was calculated by Wu [84], by Hugenholtz and Pines [85], and by Sawada [86]. A complete next-to-next-to-leading order result was obtained by Braaten and Nieto [81] using effective-field theory methods. The result depends not only on the scattering length  $a$ , but also on an energy-independent term in the scattering amplitude for  $3 \rightarrow 3$  scattering. The result is

$$\begin{aligned} \mathcal{E}(n) = & \frac{2\pi a n^2}{m} \left[ 1 + \frac{128}{15\sqrt{\pi}} \sqrt{na^3} \right. \\ & \left. + \left( \frac{32\pi - 24\sqrt{3}}{3} \log na^3 + \mathcal{G} \right) na^3 \right], \end{aligned} \quad (215)$$

where  $\mathcal{G}$  is a constant involving the coupling  $g_3$ . It was already realized by Hugenholtz and Pines that physical quantities depend on other quantities than the  $s$ -wave scattering length  $a$ . These effects are referred to as nonuniversal effects and are mimicked by e.g. the terms  $\frac{1}{4} h [\nabla(\psi^\dagger \psi)]^2$  and  $g_3 (\psi^\dagger \psi)^3$  in Eq. (214). A detailed discussion of nonuniversal effects involving these terms and a comparison with diffusion Monte Carlo calculations [88] can be found in Ref. [87].

We now rederive the first two terms in the expansion Eq. (215) using the effective nonrelativistic Lagrangian Eq. (214). The first term is the mean-field result, while the second arises from a one-loop calculation. The complex field is written as  $\psi = v + \tilde{\psi}$ , where  $v = \langle \psi \rangle$  is its expectation value and  $\tilde{\psi}$  is a fluctuating quantum field with  $\langle \tilde{\psi} \rangle = 0$ . The fluctuating field is written as

$\tilde{\psi} = \frac{1}{\sqrt{2}}(\psi_1 + i\psi_2)$ , where  $\psi_1$  and  $\psi_2$  are real fields. To second order in the fluctuations, one finds

$$\mathcal{L}^{(0)} = \mu_{\text{NR}}v^2 - \frac{1}{4}gv^4, \quad (216)$$

$$\mathcal{L}^{(1)} = \frac{vX}{\sqrt{2}m}\psi_1, \quad (217)$$

$$\begin{aligned} \mathcal{L}^{(2)} = & \frac{1}{2}(\dot{\psi}_1\psi_2 - \psi_1\dot{\psi}_2) + \frac{1}{4m}\psi_1(\nabla^2 + Y)\psi_1 \\ & + \frac{1}{4m}\psi_2(\nabla^2 + X)\psi_2, \end{aligned} \quad (218)$$

where the superscript indicates the power of the field, a dot means a time derivative,  $X = 2m(\mu_{\text{NR}} - \frac{1}{2}gv^2)$ , and  $Y = 2m(\mu_{\text{NR}} - \frac{3}{2}gv^2)$ . The propagator matrix is

$$D(\omega, p) = \frac{i}{\omega^2 - E^2(p) + i\epsilon} \begin{pmatrix} \frac{1}{2m}(p^2 - X) & -i\omega \\ i\omega & \frac{1}{2m}(p^2 - Y) \end{pmatrix}, \quad (219)$$

where the spectrum is

$$E(p) = \frac{1}{2m}\sqrt{(p^2 - X)(p^2 - Y)}. \quad (220)$$

The thermodynamic potential in the mean-field approximation is as usual given by minus the static part of the Lagrangian,

$$\Omega_0(\mu_{\text{NR}}, v) = -\mu_{\text{NR}}v^2 + \frac{1}{4}gv^4. \quad (221)$$

The minimum of  $\Omega_0(\mu_{\text{NR}}, v)$  is  $v_0 = \sqrt{\frac{2\mu_{\text{NR}}}{g}}$ . At the minimum  $v_0$ ,  $X = 0$  and Eq. (220) reduces to the Bogoliubov spectrum  $E_p = \frac{p}{2m}\sqrt{p^2 + 4m\mu_{\text{NR}}}$ . The dispersion relation is linear for small momenta,  $p^2 \ll 4m\mu_{\text{NR}}$ , and that of a free nonrelativistic particle for large momenta,  $p^2 \gg 4m\mu_{\text{NR}}$ .

In order to calculate the NLO corrections to the thermodynamic quantities, we need a few divergent loop integrals. We use dimensional regularization to regulate these integrals. The integrals needed were introduced in Ref. [89] and are of the form

$$I_{m,n}(M^2) = \Lambda^{2\epsilon} \int \frac{d^d p}{(2\pi)^d} \frac{p^{2m}}{p^n (p^2 + M^2)^{\frac{n}{2}}}, \quad (222)$$

They satisfy the recursion relation

$$\frac{dI_{m,n}(M^2)}{dM^2} = -\frac{1}{2}nI_{m+1,n+2}(M^2), \quad (223)$$

which follows directly from the definition Eq. (222). Evaluating the integrals in dimensional regularization, we find

$$\begin{aligned} I_{m,n}(M^2) = & \frac{M^{3+2m-2n}}{(4\pi)^{\frac{d}{2}}} \left(\frac{\Lambda}{M}\right)^{2\epsilon} \\ & \times \frac{\Gamma(\frac{d-n}{2} + m)\Gamma(n - m - \frac{d}{2})}{\Gamma(\frac{n}{2})\Gamma(\frac{d}{2})}. \end{aligned} \quad (224)$$

We specifically need

$$I_{0,-1}(M^2) = \frac{16}{15} \frac{M^5}{(4\pi)^2} [1 + \mathcal{O}(\epsilon)], \quad (225)$$

$$I_{1,1}(M^2) = \frac{16M^3}{3(4\pi)^2} [1 + \mathcal{O}(\epsilon)]. \quad (226)$$

The integrals are finite in the limit  $d \rightarrow 3$  reflecting that the ultraviolet divergences are powerlike.

The NLO pressure is given by the NLO thermodynamic potential evaluated at the classical minimum  $v_0$  cf. Eq. (77). This is convenient since  $X = 0$ . The NLO pressure then becomes

$$\begin{aligned} \mathcal{P}(\mu_{\text{NR}}) = & -\Omega_0(\mu_{\text{NR}}, v_0) - \Omega_1(\mu_{\text{NR}}, v_0) \\ = & \frac{\mu_{\text{NR}}^2}{g} - \frac{1}{2} \int_p E(p) \\ = & \frac{\mu_{\text{NR}}^2}{g} - \frac{1}{4m} I_{0,-1}(M^2) \\ = & \frac{\mu_{\text{NR}}^2}{g} \left[ 1 - \frac{16(4m)^{\frac{3}{2}} \sqrt{\mu_{\text{NR}} g^2}}{15(4\pi)^2} \right], \end{aligned} \quad (227)$$

where  $M^2 = 4m\mu_{\text{NR}}$ , and we have used Eq. (225). The number density is then given by

$$n(\mu_{\text{NR}}) = \frac{2\mu_{\text{NR}}}{g} - \frac{1}{2} I_{1,1}(M^2), \quad (228)$$

where we have used the recursion relation Eq. (223). We can invert Eq. (228) to obtain the chemical potential in terms of the number density. To the order we are calculating, we can make the substitution  $\mu_{\text{NR}} \rightarrow \frac{1}{2}gn$  in the loop integral  $I_{1,1}(M^2)$ . This yields

$$\begin{aligned} \mu_{\text{NR}}(n) = & \frac{1}{2}gn + \frac{1}{4}gI_{1,1}(2mgn) \\ = & \frac{4\pi an}{m} \left[ 1 + \frac{32}{3\sqrt{\pi}} \sqrt{na^3} \right], \end{aligned} \quad (229)$$

where we have used Eq. (226) and  $g = \frac{8\pi a}{m}$  in the last line. The energy density is then

$$\begin{aligned} \mathcal{E}(n) = & -\mathcal{P} + \mu_{\text{NR}}n \\ = & \frac{1}{4}gn^2 + \frac{1}{4m} I_{0,-1}(2mgn). \end{aligned} \quad (230)$$

Note that, to the order we are calculating, the terms involving  $I_{1,1}(\mu_{\text{NR}})$  cancel in final result for the energy density. Using the result Eq. (225) for the integral and the expression for  $g$  in terms of the  $s$ -wave scattering length, we obtain the result of Lee, Huang and Yang [82, 83],

$$\mathcal{E}(n) = \frac{2\pi an^2}{m} \left[ 1 + \frac{128}{15\sqrt{\pi}} \sqrt{na^3} \right]. \quad (231)$$

## B. Nonrelativistic limit of $\chi$ PT

In this section, we take the nonrelativistic limit of chiral perturbation theory in order to make contact with the theory of dilute Bose gases discussed in the previous section. In order to do so, we introduce the nonrelativistic

chemical potential  $\mu_{\text{NR}}$  by writing  $\mu_I = m_\pi + \mu_{\text{NR}}$ , where  $m_\pi$  is the physical pion mass. In a consistent calculation,  $m_\pi$  must be calculated to the same order in the low-energy expansion as the pressure itself. Expanding the pressure Eq. (180) to order  $\mu_{\text{NR}}^{5/2}$ , we obtain

$$\begin{aligned} \mathcal{P} = & 2f^2\mu_{\text{NR}}^2 \left\{ 1 - \frac{3}{2} \frac{\delta m_\pi^2}{m_{\pi,0}^2} + [32L_1^r + 32L_2^r + 16L_3^r - 40L_4^r - 20L_5^r + 80L_6^r + 40L_8^r \right. \\ & + \left. \frac{1}{(4\pi)^2} \left( \frac{11}{4} \log \frac{\Lambda^2}{m_{\pi,0}^2} + \frac{1}{2} \log \frac{\Lambda^2}{m_{K,0}^2} + \frac{5}{36} \log \frac{\Lambda^2}{m_{\eta,0}^2} + \frac{4}{9} \right) \right] \frac{m_{\pi,0}^2}{f^2} \\ & + \left. \left[ -8L_4^r + 48L_6^r + \frac{1}{(4\pi)^2} \left( \log \frac{\Lambda^2}{m_{K,0}^2} + \frac{1}{3} \log \frac{\Lambda^2}{m_{\eta,0}^2} \right) \right] \frac{\tilde{m}_{K,0}^2}{f^2} \right\} - \frac{64m_{\pi,0}\mu_{\text{NR}}^2\sqrt{4m_{\pi,0}\mu_{\text{NR}}}}{15(4\pi)^2}, \end{aligned} \quad (232)$$

where the term  $-\frac{3}{2} \frac{\delta m_\pi^2}{m_{\pi,0}^2}$  arises from distinguishing between  $m_\pi$  and  $m_{\pi,0}$  in the tree-level contribution to the pressure (which is necessary for a consistent calculation). This term can be read off Eq. (190). There is also a term linear in  $\mu_{\text{NR}}$  from the tree-level contribution to the pressure for the same reason. This term is cancelled by a similar term from loop corrections. Thus the first term in the expansion is quadratic in  $\mu_{\text{NR}}^2$ . Also note the last term in Eq. (232), which comes from the hypergeometric function. This is exactly the loop correction in Eq. (227). This yields

$$\begin{aligned} \mathcal{P} = & 2f^2\mu_{\text{NR}}^2 \left\{ 1 + [32L_1^r + 32L_2^r + 16L_3^r - 16L_4^r - 8L_5^r + 32L_6^r + 16L_8^r \right. \\ & + \left. \frac{1}{(4\pi)^2} \left( \frac{7}{2} \log \frac{\Lambda^2}{m_{\pi,0}^2} + \frac{1}{2} \log \frac{\Lambda^2}{m_{K,0}^2} + \frac{1}{18} \log \frac{\Lambda^2}{m_{\eta,0}^2} + \frac{4}{9} \right) \right] \frac{m_{\pi,0}^2}{f^2} + \left[ 16L_4^r + \frac{1}{(4\pi)^2} \log \frac{\Lambda^2}{m_{K,0}^2} \right] \frac{\tilde{m}_{K,0}^2}{f^2} \left. \right\} \\ & - \frac{64m_{\pi,0}\mu_{\text{NR}}^2\sqrt{4m_{\pi,0}\mu_{\text{NR}}}}{15(4\pi)^2}, \end{aligned} \quad (233)$$

where we have defined  $\tilde{m}_{K,0} = B_0 m_s$ , i.e. the bare kaon mass in the limit of large  $m_s$ . This form is particularly convenient if we are interested in this limit. Expanding Eq. (233) in powers of  $1/m_s$ , using Eqs. (187)–(189), we obtain

$$\mathcal{P} = 2\tilde{f}^2\mu_{\text{NR}}^2 \left\{ 1 + \left[ 8l_1^r + 8l_2^r + 2l_3^r + \frac{1}{(4\pi)^2} \left( \frac{7}{2} \log \frac{\Lambda^2}{m_{\pi,0}^2} + \frac{1}{2} \right) \right] \frac{m_{\pi,0}^2}{f^2} \right\} - \frac{64m_{\pi,0}\mu_{\text{NR}}^2\sqrt{4m_{\pi,0}\mu_{\text{NR}}}}{15(4\pi)^2}. \quad (234)$$

Using the definition Eq. (44) replacing the running parameters  $l_i^r$  by their counterparts  $\bar{l}_i$  yields

$$\mathcal{P} = \frac{m_\pi}{8\pi a} \mu_{\text{NR}}^2 \left[ 1 - \frac{32}{15\pi} \sqrt{4m_\pi\mu_{\text{NR}}a^2} \right], \quad (235)$$

where we have used the two-flavor expression for the pion mass to one-loop order and the scattering length  $a = -a_0^2/m_\pi$ , where [10]

$$m_\pi^2 = m_{\pi,0}^2 \left[ 1 - \frac{m_{\pi,0}^2}{2(4\pi)^2 f^2} \bar{l}_3 \right], \quad (236)$$

$$a_0^2 = -\frac{m_{\pi,0}^2}{4(4\pi)^2 f^2} \left[ 1 - \frac{4m_{\pi,0}^2}{3(4\pi)^2 f^2} \left( \bar{l}_1 + 2\bar{l}_2 + \frac{3}{8} \right) \right] \quad (237)$$

Calculating the isospin density and the energy density, we find

$$n_I = \frac{m_\pi}{4\pi a} \mu_{\text{NR}} \left[ 1 - \frac{8}{3\pi} \sqrt{4m_\pi\mu_{\text{NR}}a^2} \right], \quad (238)$$

$$\mathcal{E}(n_I) = m_\pi n_I + \frac{2\pi a n_I^2}{m} \left[ 1 + \frac{128}{15\sqrt{\pi}} \sqrt{n_I a^3} \right] \quad (239)$$

We can now compare our result Eq. (239) with the result of Braaten and Nieto, Eq. (215). The first term in Eq. (239) is the contribution to  $\mathcal{E}$  associated with the rest mass  $m_\pi$  of the boson. This term is absent in Eq. (215) since it is automatically removed by subtracting the rest mass energy in the nonrelativistic Lagrangian Eq. (214). Omitting this term, Eq. (239) is the same as the first and second term in Eq. (215), i.e. there is agreement to one-loop order. The last term in Eq. (215) involves



a two-loop calculation and is therefore not included in Eq. (239). See also Ref. [90] for similar results.

## X. SUMMARY AND OUTLOOK

In this paper, we have discussed various aspects of Bose condensation in QCD at finite  $\mu_I$  and  $\mu_S$  using chiral perturbation theory, which is the low-energy effective theory describing the pseudo-Goldstone bosons. We have been focusing on the pion-condensed phase mainly due to the fact that in this case it is possible to compare our predictions with those of lattice QCD. However, with relatively little effort similar results for the kaon-condensed phases can be obtained. Lattice QCD and  $\chi$ PT agree very well in the region where the latter is expected to be valid. Depending on taste, one can view this as a check of  $\chi$ PT as an effective theory of QCD or a check of the simulations. Bose-condensation in QCD is a very rich system: in the region  $\mu_I \simeq m_\pi$ , we have made contact with the dilute Bose gas and the classic results by Bogoliubov, Beliaev, Lee, Yang and Huang, and others. In the ultrarelativistic limit, the Goldstone mode is exactly linear and propagates with the speed of light. The speed of sound,  $c_s = \sqrt{\frac{\mu_I^4 - m_{\pi,0}^4}{\mu_I^4 + 3m_{\pi,0}^4}}$ , is a measure of how relativistic the system is.

The present work can be extended in several directions. Firstly, it would be interesting to calculate the thermodynamic quantities and the phase diagram to order  $\mathcal{O}(p^4)$  including electromagnetic interactions. This would require using Urech's next-to-leading order Lagrangian [48] and the evaluation of a very complicated functional determinant. In the same vein, one could calculate the meson and gauge boson masses to  $\mathcal{O}(p^4)$ . A more straight-

forward extension would be to finite temperature. In a two-flavor calculation [31], the critical line between the normal phase and the BEC phase was mapped out in the  $\mu_I$ - $T$  plane. Good agreement between  $\chi$ PT and lattice simulations was only found for temperatures up to approximately 30 MeV. Whether the inclusion of heavier mesons would improve the situation is an open question.

We have also noticed the disagreement between  $\chi$ PT and the lattice regarding the speed of sound for large values of  $\mu_I$ , which is caused by the fact that  $\chi$ PT has mesonic bound states as degrees of freedom and not quarks. This problem was addressed in Ref. [42], where the two-flavor quark-meson model was investigated at finite isospin and vanishing temperature. The model is in qualitative agreement with lattice data from the BEC to the BCS regime, suggesting that it captures the correct degrees of freedom.

## ACKNOWLEDGEMENTS

Q. Yu and H. Zhou have been supported by the Natural Science Foundation of China under Grant No.12305091, the Natural Science Foundation of Sichuan Province under Grant No.2024NSFSC1367, and the Research Fund for the Doctoral Program of the Southwest University of Science and Technology under Contract No.23zx7122 and No.24zx7117. J. O. Andersen would like to thank the Niels Bohr International Academy for kind hospitality during his stay where large part of this work was carried out. J. O. Andersen would also like to thank Prabal Adhikari and Martin Mojahed for earlier collaboration as well as Alberto Nicolis, Alessandro Podo, and Luca Santoni for useful discussions. The authors thank Bastian Brandt and Gergely Endrődi for sharing their old and updated lattice data and for discussions

- 
- [1] K. Rajagopal and F. Wilczek, *At the frontier of particle physics*, Vol. 3 (World Scientific, Singapore, p 2061) (2001).
  - [2] M. G. Alford, A. Schmitt, K. Rajagopal, and T. Schäfer, *Rev. Mod. Phys.* **80**, 1455 (2008).
  - [3] K. Fukushima and T. Hatsuda, *Rept. Prog. Phys.* **74**, 014001 (2011).
  - [4] A. W. Steiner, S. Reddy, and M. Prakash. *Phys. Rev. D* **66**, 094007 (2002).
  - [5] M. Alford and K. Rajagopal, *JHEP* **06**, 031 (2002).
  - [6] S. B. Ruster, V. Werth, M. Buballa, I. A. Shovkovy, and D. H. Rischke, *Phys. Rev. D* **72**, 034004 (2005).
  - [7] H. Abuki and T. Kunihiro, *Nucl. Phys. A* **768**, 118 (2006).
  - [8] S. Weinberg, *Physica A* **96**, 327 (1979).
  - [9] J. Gasser and H. Leutwyler, *Ann. Phys.* **158**, (142) (1984).
  - [10] J. Gasser and H. Leutwyler, *Nucl. Phys. B* **250**, 465 (1985).
  - [11] D. T. Son and M. A. Stephanov, *Phys. Rev. Lett.* **86**, 592 (2001); *Phys. Atom. Nucl.* **64**, 834 (2001).
  - [12] K. Splittorff, D. T. Son, M. A. Stephanov, *Phys. Rev. D* **64**, 016003 (2001).
  - [13] J. B. Kogut and D. Toublan, *Phys. Rev. D* **64**, 034007 (2001).
  - [14] J. B. Kogut and D. K. Sinclair, *Phys. Rev. D* **66**, 014508 (2002).
  - [15] J. B. Kogut and D. K. Sinclair, *Phys. Rev. D* **66**, 034505 (2002).
  - [16] J. B. Kogut and D. K. Sinclair, *Phys. Rev. D* **70**, 094501 (2004).
  - [17] D. K. Sinclair and J. B. Kogut, *PoSLAT 2006* **147** (2006).
  - [18] D. K. Sinclair, J. B. Kogut, *PoSLAT 2007* **225** (2007).
  - [19] B. B. Brandt and G. Endrődi, *PoS LATTICE2016*, 039 (2016).
  - [20] B. B. Brandt, G. Endrődi, and S. Schmalzbauer, *EPJ Web Conf.* **175**, 07020 (2018).
  - [21] B. B. Brandt, G. Endrődi, and S. Schmalzbauer, *Phys. Rev. D* **97**, 054514 (2018).

- [22] B. B. Brandt and G. Endrődi Phys. Rev. D **99**, 014518 (2019)
- [23] B. B. Brandt, F. Cuteri, G. Endrődi, and S. Schmalzbauer, Particles **3**, 80 (2020).
- [24] B. B. Brandt, Francesca Cuteri, and G. Endrődi, PoS LATTICE2021, 232 (2022).
- [25] B. B. Brandt, Francesca Cuteri, and G. Endrődi, JHEP **07**, 055 (2023).
- [26] R. Abbott, W. Detmold, M. Illa, A. Parreño, and R. J. Perry et al, e-Print: 2406.09273 [hep-lat].
- [27] T. D. Cohen, Phys. Rev. Lett. **91**, 222001 (2003).
- [28] S. Carignano, A. Mammarella, and M. Mannarelli, Phys. Rev. D **93**, 051503 (2016).
- [29] S. Carignano, L. Lepori, A. Mammarella, M. Mannarelli, and G. Pagliaroli Eur. Phys. J. A **53**, 35 (2017).
- [30] P. Adhikari, J. O. Andersen, and P. Kneshcke, Eur. Phys. J. C **79**, 874 (2019).
- [31] P. Adhikari, J. O. Andersen, and M. A. Mojahed, Eur. Phys. J. C **81**, 173 (2021).
- [32] P. Adhikari, J. O. Andersen, and M. A. Mojahed, Eur. Phys. J. C **81**, 449 (2021).
- [33] J. O. Andersen, Q. Yu, and H. Zhou, Phys. Rev. D **109**, 034022 (2024).
- [34] D. Ebert and K.G. Klimenko, J. Phys. G **32**, 599. (2006).
- [35] D. Ebert and K.G. Klimenko, Eur. Phys. J. C **46**, 771 (2006).
- [36] H. Abuki, T. Brauner, and H. J. Warringa, Eur. Phys. J. C **64**, 123 (2009).
- [37] T. Xia, L. He, and P. Zhuang, Phys. Rev. D **88**, 056013 (2013).
- [38] T. Khunjua, K. G. Klimenko, and R. Zhokhov, Symmetry **11**, 778 (2019).
- [39] S. S. Avancini, A. Bandyopadhyay, D. C. Duarte, and R. L. S. Farias Phys. Rev. D **100**, 116002 (2019).
- [40] T. Herpay and P. Kovács, Phys. Rev. D **78**, 116008 (2008).
- [41] A. Ayala, A. Bandyopadhyay, R. L. S. Farias, L. A. Hernandez, and J. L. Hernandez, Phys. Rev. D **107**, 074027 (2023).
- [42] R. Chiba and T. Kojo, Phys. Rev. D **109**, 076006 (2024).
- [43] R. Chiba, T. Kojo, and D. Suenaga, e-Print: 2403.02538 [hep-ph]
- [44] A. Ayala, B. S. Lopes, R. L. S. Faria, and L. C. Parra, e-Print: 2310.13130 [hep-ph].
- [45] M. S. Grønli and T. Brauner, Eur. Phys. J. C **82**, 354 (2022).
- [46] M. Mannarelli, Particles **2**, 411 (2019).
- [47] G. Ecker, J. Gasser, A. Pich, and E. de Rafael, Nucl. Phys. B **321**, 311 (1989).
- [48] R. Urech, Nucl. Phys. B **433**, 234 (1995).
- [49] R. Dashen, Phys. Rev. **183**, 1245 (1969).
- [50] U.-G. Meißner, G. Müller and S. Steininger, Phys. Lett. B **406**, 154 (1997).
- [51] M. Knecht and R. Urech, Nucl. Phys. B **519**, 329 (1998).
- [52] J. Gasser, A. Rusetsky, and I. Scimemi, Eur. Phys. J. C **32**, 97 (2003).
- [53] H. Leutwyler, Annals Phys. **235**, 165 (1994).
- [54] A. Pich, Rept. Prog. Phys. **58**, 563 (1995).
- [55] B. Gripaios, e-Print: 1506.05039 [hep-ph].
- [56] R. Penco, e-Print: 2006.16285 [hep-th].
- [57] T. Brauner, Lect. Notes Phys. 1023 (2024).
- [58] J. I. Kapusta, Phys. Rev. D **24**, 426 (1981).
- [59] H. E. Haber and H. A. Weldon Phys. Rev. D **25**, 502 (1982).
- [60] J. Bijnens, G. Colangelo, and G. Ecker, Ann. Phys. **280**, 100 (2000).
- [61] S. Scherer, e-Print: 0210398 [hep-ph].
- [62] M. K. Johnsrud, Master thesis, NTNU 2022. Thesis and code available at <https://github.com/martkjoh/master>.
- [63] J. Bijnens, G. Colangelo, and G. Ecker, JHEP **02** 020 (1999).
- [64] A. Nicolis and F. Piazza, JHEP **06**, 025 (2012).
- [65] A. Nicolis, R. Penco, F. Piazza, and R. Rattazzi, JHEP **06** 155 (2015).
- [66] P. A. Zyla et al. (Particle Data Group), Prog. Theor. Exp. Phys. 2020, 083C01 (2020).
- [67] J. Gasser and H. Leutwyler, Phys. Rep. **87**, 77 (1982).
- [68] A. Joyce, A. Nicolis, A. Podo, and L. Santoni, JHEP **09** 066 (2022).
- [69] I. S. Gradshteyn and I. M. Ryzhik, *Table of Integrals, Series, and Products*. Eighth edition (2014).
- [70] J. Bijnens and G. Ecker, Ann. Rev. of Nuclear and Particle Science, **64**, 149 (2014).
- [71] K. Fukushima and S. Minato, e-Print: 2411.03781 [hep-ph].
- [72] J. M. Cornwall, R. Jackiw, and E. Tomboulis, Phys. Rev. D **10**, 2428 (1974).
- [73] D.T. Son, e-Print: 0204199 [hep-ph].
- [74] C. Manuel, A. Dobado, and F. J. Llanes-Estrada, JHEP **09**, 076 (2005).
- [75] C. Manuel and F. J. Llanes-Estrada, JCAP **08** 001 (2007).
- [76] M. A. Escobedo and C. Manuel, Phys. Rev. A **82**, 023614 (2010).
- [77] S. T. Beliaev, Sov. Phys. JETP **7**, 299 (1958).
- [78] A. L. Fetter and J. D. Walecka, *Quantum Theory of Many-Particle Systems*, Dover publications (2003).
- [79] L. He, Phys. Rev. D **82**, 096003 (2010).
- [80] N. N. Bogoliubov, J. Phys. (USSR) **11**, 23 (1947).
- [81] E. Braaten and A. Nieto, Eur. Phys. J. B **11**, 143 (1999).
- [82] T. D. Lee and C. N. Yang, Phys. Rev. **105**, 1119 (1957).
- [83] T. D. Lee, K. Huang, and C. N. Yang, Phys. Rev. **106**, 1135 (1957).
- [84] T. T. Wu, Phys. Rev. **115**, 1390 (1959).
- [85] N. M. Hugenholz and D. Pines, Phys. Rev. **116**, 489 (1959).
- [86] K. Sawada, Phys. Rev. **116**, 1344 (1959).
- [87] E. Braaten, H.-W. Hammer, and S. Hermans, Phys. Rev. A **63**, 063609 (2001).
- [88] S. Giorgini, J. Boronat, and J. Casulleras, Phys. Rev. A **60**, 5129 (1999).
- [89] E. Braaten and A. Nieto Phys. Rev. B **56**, 14745 (1997).
- [90] A. Nicolis, A. Podo, and L. Santoni, JHEP **09**, 200 (2023)